

A top-down approach to uncover the hidden ligandome of low-density lipoprotein receptor-related protein 1 in cartilage

Kazuhiro Yamamoto [a], Carsten Scavenius [b], Maria M Meschis [a], Abdulrahman M E Gremida [a], Emilie H Mogensen [b], Ida B Thøgersen [b], Simone Bonelli [c], Simone D Scilabra [c], Anders Jensen [a], Salvatore Santamaria [d], Josefin Ahnström [d], George Bou-Gharios [a], Jan J Enghild [b] and Hideaki Nagase [e]

a* - *Institute of Life Course and Medical Sciences, William Henry Duncan Building, *University of Liverpool, 6 West Derby Street, Liverpool L7 8TX, United Kingdom*
b* - *Department of Molecular Biology and Genetics, *Aarhus University, Aarhus 8000, Denmark*
c* - *Fondazione RiMED - ISMETT via Ernesto Tricomi 5, *Palermo 90127, Italy*
d* - *Department of Immunology and Inflammation, *Imperial College London, Du Cane Road, London W12 0NN, United Kingdom*
e* - *Kennedy Institute of Rheumatology, *University of Oxford, Headington, Oxford OX3 7FY, United Kingdom*

Corresponding author. ***Kazuhiro.yamamoto@liverpool.ac.uk.***
https://*doi.org/10.1016/j.matbio.2022.08.007*

Abstract

The low-density lipoprotein receptor-related protein 1 (LRP1) is a cell-surface receptor ubiquitously expressed in various tissues. It plays tissue-specific roles by mediating endocytosis of a diverse range of extracellular molecules. Dysregulation of LRP1 is involved in multiple conditions including osteoarthritis (OA) but little information is available about the specific profile of direct binding partners of LRP1 (ligandome) for each tissue, which would lead to a better understanding of its role in disease states. Here, we investigated adult articular cartilage where impaired LRP1-mediated endocytosis leads to tissue destruction. We used a top-down approach involving proteomic analysis of the LRP1 interactome in human chondrocytes, direct binding assays using purified LRP1 and ligand candidates, and validation in LRP1-deficient fibroblasts and human chondrocytes, as well as a novel *Lrp1* conditional knockout (KO) mouse model. We found that inhibition of LRP1 and ligand interaction results in cell death, alteration of the entire secretome and transcriptional modulations in human chondrocytes. We identified a chondrocyte-specific LRP1 ligandome consisting of more than 50 novel ligand candidates. Surprisingly, 23 previously reported LRP1 ligands were not regulated by LRP1-mediated endocytosis in human chondrocytes. We confirmed direct LRP1 binding of HGFAC, HMGB1, HMGB2, CEMIP, SLIT2, ADAMTS1, TSG6, IGFBP7, SPARC and LIF, correlation between their affinity for LRP1 and the rate of endocytosis, and some of their intracellular localization. Moreover, a conditional LRP1 KO mouse model demonstrated a critical role of LRP1 in regulating the high-affinity ligands in cartilage *in vivo*. This systematic approach revealed the specificity and the extent of the chondrocyte LRP1 ligandome and identified potential novel therapeutic targets for OA.

Crown Copyright © 2022 Published by Elsevier B.V. This is an open access article under the CC BY license (http://creativecommons.org/licenses/by/4.0/)

Introduction

Endocytosis is the process by which cells control the composition of their cell surface and extracellular environment and is thus essential for cellular signalling and metabolism. The low-density lipoprotein receptor-related protein 1 (LRP1, CD91) is a type 1 transmembrane protein consisting of a 515 kDa heavy-chain containing the extracellular ligand-binding domains, and a non-covalently associated 85 kDa light-chain containing a transmembrane and cytoplasmic domain. LRP1 is ubiquitously expressed in different tissues and cell types [1,2],

0945-053X/Crown Copyright © 2022 Published by Elsevier B.V. This is an open access article under the CC BY license (http://creativecommons.org/licenses/by/4.0/)

and mediates clathrin-dependent endocytosis of structurally and functionally diverse array of molecules including lipoproteins, extracellular matrix (ECM) proteins, growth factors, cell surface receptors, proteinases, proteinase inhibitors and secreted intracellular proteins [3,4]. LRP1 is not only involved in ligand uptake but also in modulation of cellular signalling pathways by binding extracellular ligands including growth factors and subsequent intracellular interaction with scaffolding and adaptor proteins. The LRP1 intracellular domain contains two tyrosine phosphorylation sites, which can directly transmit the signals [5].

Ubiquitous deletion of the *Lrp1* gene in mice results in early embryonic lethality at E13.5 [6] due to extensive haemorrhaging, resulting from a failure to recruit and maintain smooth muscle cells (SMCs) and pericytes in the vasculature [7]. The selective deletion of LRP1 in neurons [8], macrophages [9,10], hepatocytes [11,12], SMCs [13,14], endothelial cells [15] or adipocytes [16] all lead to significant phenotypic alterations. These studies revealed various biological roles of LRP1 including lipoprotein metabolism, insulin signalling, vascular wall integrity, inflammation, and the turnover of ECM components. Unsurprisingly, its dysregulation is linked to several diseases such as Alzheimer's disease, atherosclerosis, cancer, and osteoarthritis (OA) [5,17–19].

OA is a major cause of pain and disability and is the most prevalent age-related degenerative joint disease. With an expanding elderly population, OA imposes a major socio-economic burden on society [20]. Despite its prevalence, there is currently no disease-modifying OA treatment available, instead joint replacement surgery is often required during the late stages of the disease. The hallmark of OA is loss of articular cartilage, which results in impairment of joint function. Chondrocytes, as the only cell type present in articular cartilage, are essential for balancing anabolic and catabolic processes. Therefore, chondrocytes are key regulators of cartilage homeostasis and joint health. Our previous study has shown that LRP1 plays a major role in maintaining the ECM turnover of healthy adult cartilage by controlling extracellular levels of matrix-degrading metalloproteinases such as aggrecanases [21,22], collagenases [23,24], and their endogenous inhibitor tissue inhibitor of metalloproteinases (TIMP)3 [25,26]. However, this endocytic process is impaired in cartilage with OA, resulting in prolonged presence of LRP1 ligands at extracellular milieu shifting homeostatic cartilage matrix turnover to a catabolic state [19]. The impairment of LRP1 is due to an increase in the proteolytic shedding of the ectodomain of the receptor from the cell surface and we have previously identified matrix metalloproteinase 14 (MMP14) and a disintegrin and metalloproteinase 17 (ADAM17) as the major LRP1 sheddases in human OA cartilage. Importantly, inhibition of LRP1 shedding recovered the endocytic capacity of the cells and reduced ECM degradation in OA cartilage [19]. Dysregulated LRP1 shedding is also observed in various pathological conditions such as rheumatoid arthritis, systemic lupus erythematosus [27], and in cancer [28,29].

To date, more than 80 LRP1 ligands have been reported in the literature [4,30] and the list is still growing. However, very limited information is available on how LRP1 ligand profiles, i.e., its ligandome, differ in specific tissues including cartilage. This is partly due to that tightly regulated LRP1 ligands are rarely detectable in the tissue unless LRP1-mediated endocytosis is blocked [22,23,26,31]. Uncovering the depth of this "hidden" ligandome is essential to identify novel molecular interactions, and possibly therapeutic opportunities. In this study, we took a systematic top-down approach to uncover the LRP1 ligandome in healthy cartilage. Our seretome and co-immunoprecipitation analysis revealed that a number of previously reported LRP1 ligands are not regulated by LRP1-mediated endocytosis in human chondrocytes and identified more than 50 novel LRP1 interaction partners whose excessive activities exerts detrimental consequences for chondrocytes and cartilage tissue integrity.

Results

Inhibition of LRP1 and ligand interaction induces chondrocyte cell detachment and death

Inhibition of LRP1-mediated endocytosis is essential to enable the identification of tightly regulated LRP1 ligands. We thus decided to block LRP1 and ligand interaction in human chondrocytes using either 10 nM soluble form of full-length LRP1 (sLRP1) or 500 nM receptor-associated protein (RAP). sLRP1 binds to LRP1 ligands and acts as a soluble decoy receptor competing with the endogenous LRP1, whereas RAP antagonises ligand binding by competitively occupying the ligand binding region of LRP1 (**Fig. 1A**). Initially, we evaluated the effect of sLRP1 and RAP on chondrocytes morphology and viability. We found that 72 h incubation with either the inhibitor or soluble receptor resulted in altered chondrocyte morphology and a significant number of the cells detaching from the plate surface (**Fig. 1B**). The cell-counting of the attached cells showed that compared to 0 h, approx. 62% and 65% of the cells were detached after 72 h incubation with sLRP1 or RAP, respectively (**Fig. 1C**). The MTS cell metabolic assay further showed that compared to 0-h, approx. 54% and 58% of the cells were dead after 72 h incubation with sLRP1 or RAP, respectively (**Fig. 1D**). The time-dependent effect of sLRP1 and

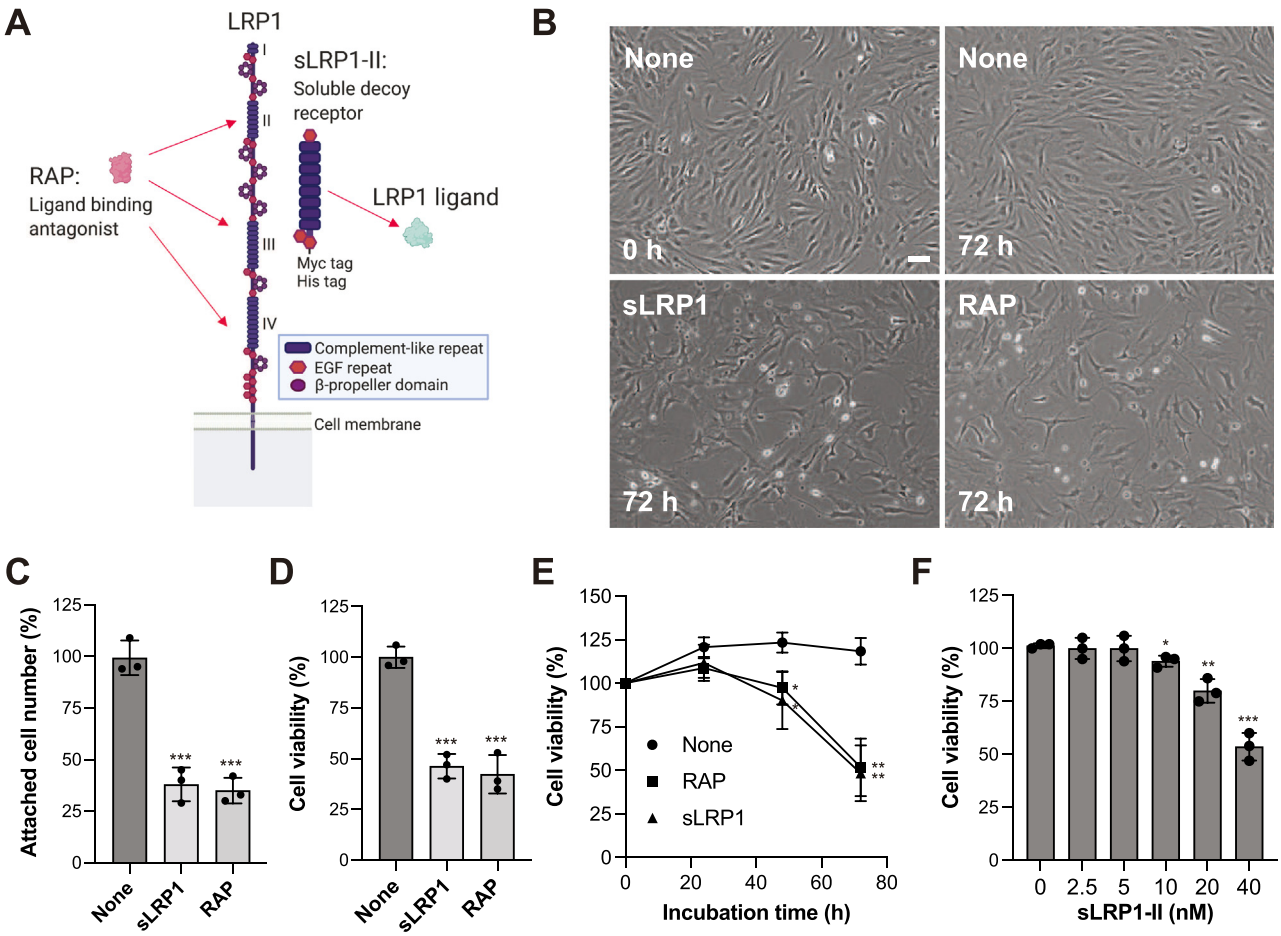


Fig. 1. Inhibition of LRP1 and ligand interaction induces chondrocyte cell detachment and death.
A, Schematic representation of membrane-bound LRP1, receptor-associated protein (RAP), and the soluble form of LRP1 ligand binding cluster II (sLRP1-II). sLRP1−II containing a C-terminal 6xHis/c-Myc tag and c-Myc antibody. RAP antagonises LRP1 ligands by binding to the ligand binding clusters II−IV whereas sLRP1 binds to LRP1 ligands and acts as a soluble decoy receptor. *B-E*, Human chondrocytes from three different donors (M1, F1 and F2) were cultured with serum-free DMEM in the absence or presence of 10 nM full-length sLRP1 or 500 nM RAP for 0-72 h. *B*, Cell morphology was observed and imaged after 72 h incubation. Scale bar, 30 μm. *C*, Attached cell number was measured using hemocytometer and the cell number at each condition was expressed as a % of the cell number at 0 h. *D* and *E*, Cell viability was measured using the MTS assay and analysed as in *C*. Data are expressed as the mean ± *SD*. *F*, Human chondrocytes from three different donors (M1, F1 and F2) were cultured with serum-free DMEM in the absence or presence of 0−40 nM sLRP1-II for 24 h. Cell viability was measured using the MTS assay and expressed as in *C*. Circles represent individual cartilage donors and bars show the mean ± *SD*. *, $p < 0.05$, **, $p < 0.01$, ***, $p < 0.001$ by 2-tailed Student's t test.

RAP on the cell detachment (**Suppl Fig. 1A**) and cell death (Fig. 1E) indicates that the accumulation of LRP1 ligands gradually changes chondrocyte cell behaviors leading to cell death.

The ligand binding regions in LRP1 lie in four clusters (clusters I-IV), containing 2 to 11 individual ligand binding cysteine-rich complement-like repeats. Clusters II and IV are considered to be responsible for most ligand binding [32−34] and our previous studies have demonstrated the importance of cluster II for the binding of a disintegrin and metalloproteinase with thrombospondin motifs (ADAMTS) 4, ADAMTS5 [21], MMP13 [23] and TIMP3 [35]. Thus, we next tested the effect of the soluble form of LRP1 ligand-binding cluster II (sLRP1-II) on chondrocyte cell death. After 24-h incubation with 40 nM sLRP1-II, approx. 60% of the cells were dead compared to 0-h (Fig. 1F), indicating that sLRP1-II also blocks the interaction between LRP1 and its ligands, whose accumulation is detrimental to the cells. We further examined the dose-dependent effect of sLRP1-II and found that 24 h incubation with 20 nM and 10 nM sLRP1-II resulted in approx. 25% and 9% of cell death, respectively, whereas 5 nM and 2.5 nM sLRP1-II showed negligible effect (Fig. 1F). Similar results were obtained for the cell detachment

(**Suppl Fig. 1B)**. The highest concentration of sLRP1-II that did not induce the cell death or detachment up to 24 h incubation (5 nM) was thus employed for LRP1 ligand screening. We further confirmed that after 24 h incubation with chondrocytes approx. 55%, 45% and 51% of intact form of RAP (500 nM), sLRP1 (10 nM) and sLRP1-II (5 nM), respectively, remained in the medium (**Suppl Fig. 2).**

Alteration of the entire chondrocyte secretome by inhibition of LRP1-mediated endocytosis

We performed a complete chondrocyte secretome analysis to determine the effect of inhibition of LRP1-mediated endocytosis and identify LRP1 ligands whose excess activity exerts detrimental consequences for chondrocytes. This analysis identified 603 proteins including 198 secreted, 428 intracellular and 21 transmembrane (excluding LRP1) molecules according to the Uniprot annotation. Treatment of 5 nM sLRP1-II for 24-h resulted in significant alteration of 448 proteins including the molecules found in the medium of chondrocytes only in the presence or absence of sLRP1-II, or the molecules with an adjusted p-value corrected for a false discovery rate (FDR) <0.01. Thirty-nine secreted, 305 intracellular and 10 transmembrane proteins were increased, whereas 103 secreted, 15 intracellular and 7 transmembrane proteins were decreased by the sLRP1-II treatment (**Fig. 2A**–**C** and **Suppl Table 1**). The secreted proteins significantly (>2.5-fold difference, FDR<0.01 and p-value <0.05) increased or decreased in the presence of sLRP1-II are listed on **Table 1** or **Table 2**, respectively. Among the 39 secreted proteins increased by the sLRP1-II treatment, only 10 molecules have previously been reported as LRP1 ligands (**Fig. 2C**). Unexpectedly, a total of 23 previously reported LRP1 ligands were decreased (14) or unaltered (9) by the sLRP1-II treatment (**Fig. 2D**). These results suggest that the identified chondrocyte LRP1 ligandome consists of mostly novel ligands and that the 23 previously reported LRP1 ligands are not regulated by LRP1-mediated endocytosis in human chondrocytes.

Inhibition of LRP1-mediated endocytosis induces transcriptional modulations

It has been reported that RAP increases mRNA levels of pro-inflammatory mediators such as TNFα, interleukin-6 and C–C motif chemokine ligand 2 in macrophages [36]. We next investigated the effect of inhibition of LRP1-mediated endocytosis on transcriptional modulation of several LRP1 ligands and a non-ligand. Our recent [24] study identified MMP1, a collagenase highly elevated in knee joint and synovial fluid from patients with arthritis [37,38], as an LRP1 ligand. We found that endogenously produced MMP1 was not detectable in the medium of chondrocytes in the absence of RAP, whereas it was increased after 24 h-incubation with 200 nM RAP (**Fig. 3A**). Similar results were obtained for MMP3 (**Fig. 3B**), which is not a LRP1 ligand but relevant to arthritis pathogenesis [37,38]. Notably, the quantitative PCR analysis revealed that mRNA levels of MMP1 and MMP3 in human chondrocytes are increased time-dependently in the presence of 200 nM RAP or 10 nM sLRP1 (**Fig. 3C and D**). In contrast, denatured sLRP1 did not affect their mRNA expression, suggesting that functional sLRP1 is required for upregulation of mRNA levels of these proteinases. Similar results were obtained for other LRP1 ligands, MMP13 and ADAMTS4 (**Fig. 3E and F**), whereas mRNA levels of ADAMTS5 or TIMP3 were not affected by inhibition of LRP1-mediated endocytosis (**Fig. 3G and H**). These studies suggest that excessive activity of LRP1 ligands alters transcription of several molecules. In addition, a fraction of the molecules increased upon sLRP1-II treatment in our secretome analysis (**Fig. 2**) might not be LRP1 ligands but due to transcriptional upregulation.

The chondrocyte LRP1 ligandome comprises a variety of novel ligands

To enrich and identify molecules that directly interact with LRP1, we have employed co-immunoprecipitation assay for sLRP1-II containing a C-terminal 6xHis/c-Myc tag and c-Myc antibody. The isolation of LRP1 ligands using this method was first validated using ADAMTS5 (**Suppl Fig. 3**). Purified ADAMTS5 (5 nM) was mixed with 5 nM sLRP1-II and anti-c-Myc antibody-coupled paramagnetic beads, recognising sLRP1-II. Complexes of sLRP1-II, ADAMTS5 and the magnetic beads were then isolated using a magnetic separator. Most of ADAMTS5 and sLRP1-II were detected in the bound fraction (**Suppl Fig. 3A**). As expected, RAP competitively inhibited ADAMTS5 binding to sLRP1-II. Since LRP1 ligands dissociate from LRP1 in the early endosome due to acidic conditions, we have tested whether acidic conditions (pH 3.0) can dissociate molecules bound to sLRP1-II/anti-c-Myc antibody complexes. As expected, ADAMTS5 were eluted under acidic conditions as effectively as 1% sodium dodecyl sulphate (SDS) or 100 nM RAP (**Suppl Fig. 3B**). To identify LRP1 ligands produced by human chondrocytes, cells were incubated without (control) or with 5 nM sLRP1-II for 24 h and the molecules bound to sLRP1-II were isolated as described above (**Fig. 4A**). The molecules isolated by the same procedure without sLRP1-II were considered as a negative control and used to estimate a fold-difference for the ligand identification. Western blot analysis of the isolated proteins using anti-His

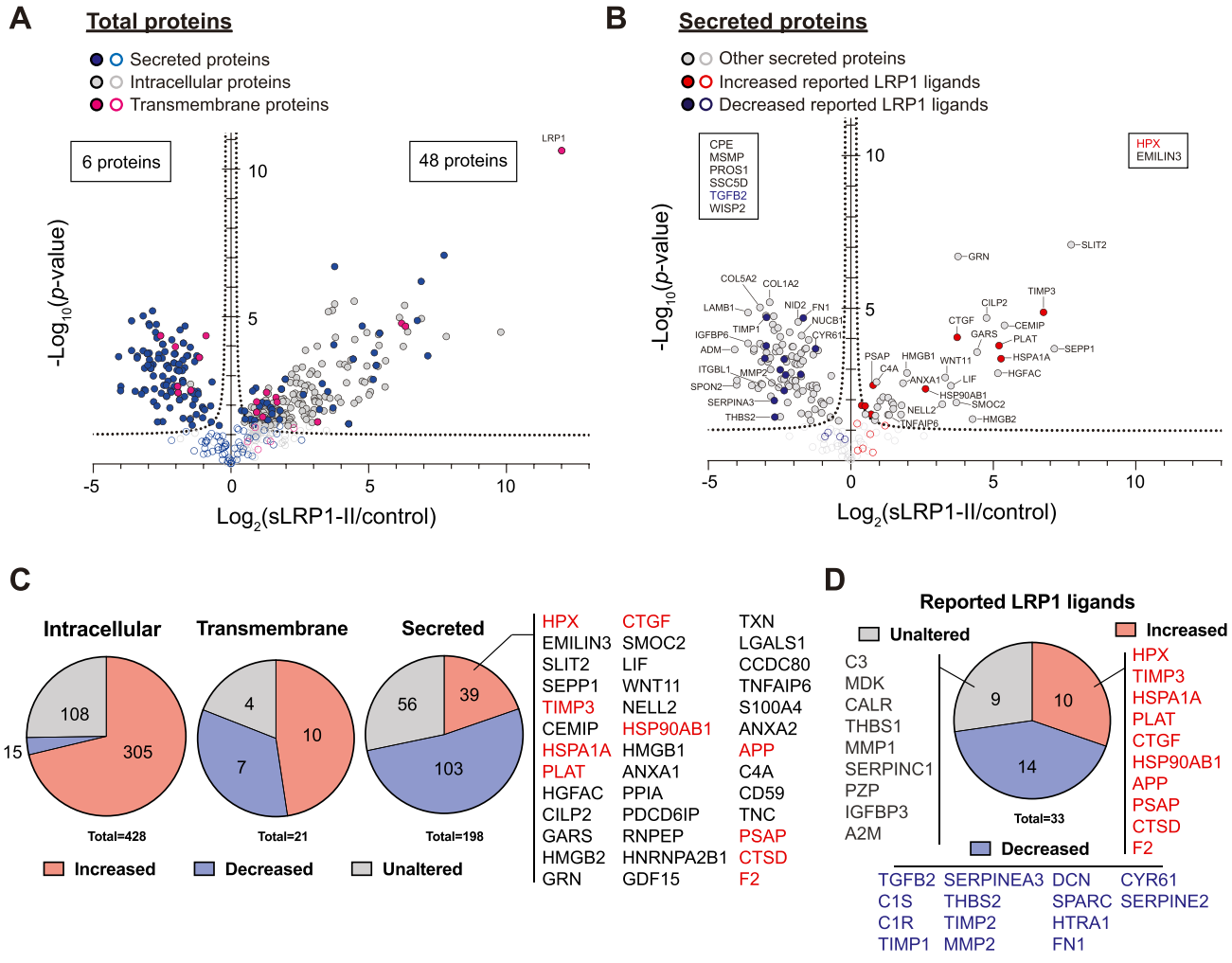


Fig. 2. Alteration of the entire chondrocyte secretome by inhibition of LRP1-mediated endocytosis.

Human chondrocytes from four different donors (M1, M2, F1 and F2) were incubated with serum-free DMEM in the absence or presence of 5 nM sLRP1-II for 24 h. The conditioned medium was collected and centrifuged to remove cell debris. The supernatant was then subjected to mass spectrometry-based protein identification. *A*, Volcano plot showing the $-\log_{10}$ of *p*-values *versus* the log2 of protein ratio for all proteins identified in the medium of chondrocytes in the presence and absence of sLRP1-II. The proteins identified in all 4 biological replicates of sLRP1-II-treated cells, but only in 0-1 replicates of untreated control cells were categorized as ON molecules and the number of ON molecules shown in the insert at the top right corner of the plot. Conversely, the proteins identified in all 4 replicates of control cells, but only in 0-1 replicates of sLRP1-II-treated cells were categorized as OFF molecules and the number of OFF molecules shown in the insert at the top left corner of the plot. Blue, grey and pink circles represent secreted, intracellular and transmembrane proteins, respectively. Threshold for adjusted *p*-values (FDR <0.01) was shown as dotted curve. Closed and open circles represents significantly (*p*-value <0.05) and non-significantly regulated molecules, respectively. *B*, Volcano plot showing the $-\log_{10}$ of *p*-values *versus* the $\log_2$ of protein ratio for only secreted proteins. Left and right top panels show OFF and ON secreted proteins, respectively. Previously reported LRP1 ligands increased or decreased in the presence of sLRP1-II are highlighted in red or blue, respectively. *C*, Pie chart showing number of secreted, intracellular, and transmembrane proteins that were significantly (ON/OFF proteins or FDR <0.01) increased (red) or decreased (blue), or unaltered (grey) in the presence of sLRP1-II. Gene name for the significantly increased secreted proteins were listed and previously reported LRP1 ligands highlighted in red. *D*, Pie chart showing previously reported LRP1 ligands with their gene name that were significantly increased (red) or decreased (blue), or unaltered (grey) in the presence of sLRP1-II (For interpretation of the references to color in this figure legend, the reader is referred to the web version of this article.).

tag antibodies confirmed the isolation of sLRP1-II added to the culture (**Suppl Fig. 4**).

Mass spectrometry analysis identified 276 molecules co-immunoprecipitated with sLRP1-II from the medium of human chondrocytes. These molecules include 50 secreted proteins, whereas the remainder of the molecules are either intracellular or transmembrane proteins according to the Uniprot annotation

Table 1. Secreted proteins increased in medium of human chondrocytes after 24 h incubation with sLRP1-II.

Description	Gene name	Accession	Ratio (sLRP1-II vs control)	p-value
Proteins identified only with sLRP1-II				
*Hemopexin	HPX	P02790		
EMILIN-3	EMILIN3	Q9NT22		
Proteins >2.5 fold increased with sLRP1-II				
Slit homolog 2 protein	SLIT2	O94813	212.84	8.41E-08
Selenoprotein P	SEPP1	P49908	141.57	2.12E-04
*Metalloproteinase inhibitor 3	TIMP3	P35625	108.93	1.35E-05
Cell migration-inducing and hyaluronan-binding protein	CEMIP	Q8WUJ3	42.18	3.65E-05
*Heat shock 70 kDa protein 1A	HSPA1A	P0DMV8	38.78	4.54E-04
*Tissue-type plasminogen activator	PLAT	P00750	36.90	1.67E-04
Hepatocyte growth factor activator	HGFAC	Q04756	35.81	1.34E-03
Cartilage intermediate layer protein 2	CILP2	Q8IUL8	27.20	2.09E-05
Glycine−tRNA ligase	GARS	P41250	21.57	2.75E-04
High mobility group protein B2	HMGB2	P26583	19.39	4.26E-02
Progranulin	GRN	P28799	13.59	2.02E-07
*Connective tissue growth factor	CTGF	P29279	13.35	9.00E-05
SPARC-related modular calcium-binding protein 2	SMOC2	Q9H3U7	13.01	1.25E-02
Leukemia inhibitory factor	LIF	P15018	11.46	3.51E-03
Protein Wnt-11	WNT11	O96014	9.92	1.86E-03
Protein kinase C-binding protein NELL2	NELL2	Q99435	9.30	1.40E-02
*Heat shock protein HSP 90-beta	HSP90AB1	P08238	6.19	4.40E-03
High mobility group protein B1	HMGB1	P09429	3.92	1.31E-03
Annexin A1	ANXA1	P04083	3.58	2.86E-03
Peptidyl-prolyl cis-trans isomerase A	PPIA	P62937	3.44	1.53E-02
Programmed cell death 6-interacting protein	PDCD6IP	Q8WUM4	3.43	5.13E-02
Aminopeptidase B	RNPEP	Q9H4A4	3.39	3.03E-02
Heterogeneous nuclear ribonucleoproteins A2/B1	HNRNPA2B1	P22626	2.82	1.99E-02
Growth/differentiation factor 15	GDF15	Q99988	2.82	1.42E-02
Thioredoxin	TXN	P10599	2.73	1.22E-02
Galectin-1	LGALS1	P09382	2.53	3.15E-02

All proteins >2.5 fold increased with sLRP1-II are FDR <0.01.
*LRP1 ligands already reported.

(**Suppl Table 2**), supporting a notion that LRP1 plays a role in the clearance of cellular debris [30]. Among the 50 secreted proteins identified, 14 molecules were previously reported LRP1 ligands, while 36 molecules were novel LRP1 ligand candidates (**Fig. 4B and Table 3**). These 36 ligand candidates included 21 proteins that were significantly increased (16) or decreased (5) (FDR<0.01) by sLRP1-II treatment in the secretome analysis, respectively. The Protein ANalysis THrough Evolutionary Relationships (PANTHER) [39] gene ontology analysis on biological processes of these molecules that interact with LRP1 showed that 27, 19 and 16 of them are involved in "Cellular processes", "Biological regulation" and "Response to stimulus and metabolic process", respectively (**Suppl Fig. 5A**). The Search Tool for Retrieval of Interacting Genes/Proteins (STRING) analysis [40] of protein-protein interactions further revealed functional and physical interactions of these molecules illustrated in (**Suppl Fig. 5B**).

Newly identified LRP1 ligands exhibit a wide range of affinities

Based on the mass-spectrometry scores, reported pathophysiological functions and a feasibility to obtain purified proteins, we selected 12 proteins for further characterization: hepatocyte growth factor activator (HGFA, gene name: HGFAC), inflammatory mediators high-mobility group protein (HMG)B1 and HMGB2, hyaluronan-binding protein CEMIP (also known as KIAA1199 and HYBID), slit homolog 2 protein (SLIT2), secreted growth factor progranulin (gene name: GRN), proteoglycanase ADAMTS1, which was increased in medium of HEK293 cells treated with RAP in our previous study [41], tumour necrosis factor (TNF)-inducible gene 6 protein (TSG6, gene name: TNFAIP6), ECM glycoprotein fibulin1C (gene name: FBLN1), insulin-like growth factor-binding protein (IGFBP)7, secreted protein acidic and rich in cysteine (SPARC, also known as osteonectin), which is previously identified as one of the proteins co-isolated with sLRP1 binding clusters II and IV [30] but no evidence of direct LRP1 binding provided, leukemia inhibitory factor (LIF) and cathepsin D, which has been reported to bind to β-chain of LRP1 [42]. To confirm their direct binding and estimate their affinity for LRP1, solid-phase binding assay were performed using purified ligand candidates and full-length sLRP1. We found that HMGB1 (6.4 nM), HMGB2 (3.9 nM), CEMIP (2.6 nM), SLIT2 (2.0 nM), ADAMTS1 (20.2 nM),

Table 2. Secreted molecules decreased in medium of human chondrocytes after 24-h incubation with sLRP1-II.

Description	Gene name	Accession	Ratio (control vs sLRP1-II)	p-value
Proteins identified only without sLRP1-II				
Vitamin K-dependent protein S	PROS1	P07225		
Prostate-associated microseminoprotein	MSMP	Q1L6U9		
Soluble scavenger receptor cysteine-rich domain-containing protein SSC5D	SSC5D	A1L4H1		
Carboxypeptidase E	CPE	P16870		
*Transforming growth factor beta-2 proprotein	TGFB2	P61812		
WNT1-inducible-signaling pathway protein 2	WISP2	O76076		
Proteins >2.5 fold deceased with sLRP1-II				
ADM	ADM	P35318	16.80	1.60E-17
Spondin-2	SPON2	Q9BUD6	16.11	7.84E-17
Complement factor H	CFH	P08603	15.91	1.22E-16
Laminin subunit beta-1	LAMB1	P07942	12.19	6.52E-13
Insulin-like growth factor-binding protein 6	IGFBP6	P24592	12.17	6.72E-13
Collagen alpha-1(XV) chain	COL15A1	P39059	11.12	7.54E-12
Pigment epithelium-derived factor	SERPINF1	P36955	10.60	2.51E-11
Extracellular superoxide dismutase [Cu-Zn]	SOD3	P08294	10.48	3.28E-11
Olfactomedin-like protein 2B	OLFML2B	Q68BL8	9.47	3.41E-10
Mimecan	OGN	P20774	9.12	7.50E-10
Collagen alpha-2(V) chain	COL5A2	P05997	9.09	8.17E-10
Chitinase-3-like protein 2	CHI3L2	Q15782	8.84	1.43E-09
Cartilage oligomeric matrix protein	COMP	P49747	8.77	1.72E-09
Integrin beta-like protein 1	ITGBL1	O95965	8.59	2.55E-09
Adipocyte enhancer-binding protein 1	AEBP1	Q8IUX7	8.19	6.49E-09
*Complement C1s subcomponent	C1S	P09871	8.10	7.87E-09
Extracellular matrix protein 1	ECM1	Q16610	7.89	1.30E-08
*Complement C1r subcomponent	C1R	P00736	7.80	1.59E-08
Laminin subunit gamma-1	LAMC1	P11047	7.76	1.75E-08
*Metalloproteinase inhibitor 1	TIMP1	P01033	7.74	1.83E-08
C-type lectin domain family 11 member A	CLEC11A	Q9Y240	7.49	3.24E-08
Fibrillin-1	FBN1	P35555	7.48	3.29E-08
Collagen alpha-2(I) chain	COL1A2	P08123	7.19	6.50E-08
EGF-containing fibulin-like extracellular matrix protein 2	EFEMP2	O95967	7.10	7.97E-08
Cystatin-C	CST3	P01034	7.05	8.88E-08
Olfactomedin-like protein 3	OLFML3	Q9NRN5	7.01	9.74E-08
Thrombospondin-3	THBS3	P49746	6.83	1.47E-07
Follistatin-related protein 1	FSTL1	Q12841	6.64	2.29E-07
Insulin-like growth factor-binding protein 4	IGFBP4	P22692	6.52	3.04E-07
*Alpha-1-antichymotrypsin	SERPINA3	P01011	6.45	3.58E-07
Ribonuclease 4	RNASE4	P34096	6.42	3.81E-07
*Thrombospondin-2	THBS2	P35442	6.33	4.64E-07
Lumican	LUM	P51884	6.19	6.40E-07
Laminin subunit alpha-4	LAMA4	Q16363	6.12	7.60E-07
Sulfhydryl oxidase 1	QSOX1	O00391	5.87	1.35E-06
Beta-2-microglobulin	B2M	P61769	5.76	1.73E-06
EGF-containing fibulin-like extracellular matrix protein 1	EFEMP1	Q12805	5.65	2.25E-06
*Metalloproteinase inhibitor 2	TIMP2	P16035	5.58	2.65E-06
Chitinase-3-like protein 1	CHI3L1	P36222	5.56	2.73E-06
Fibronectin type III domain-containing protein 1	FNDC1	Q4ZHG4	5.56	2.74E-06
Fibromodulin	FMOD	Q06828	5.40	3.95E-06
Biglycan	BGN	P21810	5.26	5.45E-06
Collagen alpha-1(XII) chain	COL12A1	Q99715	5.07	8.54E-06
*72 kDa type IV collagenase	MMP2	P08253	5.06	8.76E-06
*Decorin	DCN	P07585	5.04	9.16E-06
Collagen and calcium-binding EGF domain-containing protein 1	CCBE1	Q6UXH8	4.90	1.25E-05
*SPARC	SPARC	P09486	4.87	1.34E-05
Procollagen C-endopeptidase enhancer 2	PCOLCE2	Q9UKZ9	4.79	1.62E-05
Cartilage intermediate layer protein 1	CILP	O75339	4.66	2.20E-05
Collagen alpha-2(IV) chain	COL4A2	P08572	4.57	2.71E-05
Proteoglycan 4	PRG4	Q92954	4.47	3.39E-05
Tetranectin	CLEC3B	P05452	4.41	3.88E-05
Testican-1	SPOCK1	Q08629	4.27	5.36E-05
Clusterin	CLU	P10909	4.19	6.52E-05
Collagen alpha-2(VI) chain	COL6A2	P12110	4.16	6.86E-05

(*continued*)

Table 2 (*Continued*)

Description	Gene name	Accession	Ratio (control vs sLRP1-II)	p-value
Inactive carboxypeptidase-like protein X2	CPXM2	Q8N436	4.15	7.07E-05
Collagen alpha-1(VI) chain	COL6A1	P12109	4.06	8.72E-05
Aggrecan core protein	ACAN	P16112	3.89	1.29E-04
Polypeptide N-acetylgalactosaminyltransferase 2	GALNT2	Q10471	3.83	1.47E-04
Ectonucleotide pyrophosphatase/phosphodiesterase family member 2	ENPP2	Q13822	3.82	1.50E-04
Dystroglycan	DAG1	Q14118	3.77	1.68E-04
Procollagen C-endopeptidase enhancer 1	PCOLCE	Q15113	3.69	2.04E-04
Insulin-like growth factor-binding protein 7	IGFBP7	Q16270	3.68	2.07E-04
Lysyl oxidase homolog 3	LOXL3	P58215	3.65	2.25E-04
Nidogen-2	NID2	Q14112	3.59	2.57E-04
Latent-transforming growth factor beta-binding protein 2	LTBP2	Q14767	3.40	3.95E-04
*Serine protease HTRA1	HTRA1	Q92743	3.38	4.12E-04
Collagen alpha-1(III) chain	COL3A1	P02461	3.36	4.35E-04
Collagen alpha-1(V) chain	COL5A1	P20908	3.34	4.58E-04
Collagen alpha-3(VI) chain	COL6A3	P12111	3.33	4.71E-04
Nucleobindin-1	NUCB1	Q02818	3.30	4.98E-04
Lactadherin	MFGE8	Q08431	3.21	6.23E-04
Plasma protease C1 inhibitor	SERPING1	P05155	3.20	6.35E-04
*Fibronectin	FN1	P02751	3.17	6.76E-04
EMILIN-1	EMILIN1	Q9Y6C2	3.05	8.93E-04
Osteomodulin	OMD	Q99983	2.97	1.08E-03
Collagen alpha-1(II) chain	COL2A1	P02458	2.80	1.57E-03
Collagen alpha-1(I) chain	COL1A1	P02452	2.78	1.67E-03
Versican core protein	VCAN	P13611	2.74	1.84E-03
Target of Nesh-SH3	IGFBP5	P24593	2.64	2.28E-03
Collagen alpha-1(XIV) chain	ABI3BP	Q7Z7G0	2.61	2.44E-03
Collagen alpha-1(XIV) chain	COL14A1	Q05707	2.55	2.83E-03
EGF-like repeat and discoidin I-like domain-containing protein 3	EDIL3	O43854	2.52	3.03E-03

All proteins >2.5 fold decreased with sLRP1-II are FDR <0.01.
*LRP1 ligands already reported.

TSG6 (11.0 nM), IGFBP7 (11.0 nM) and SPARC (41.0 nM) directly bind to immobilised LRP1 with high affinity (apparent binding constant ($K_{D,app}$) indicated in parentheses)(**Fig. 5B-E, GH and JK**). HGFA (>500 nM) and LIF (>200 nM) also directly bind to immobilised LRP1 but their affinities for LRP1 were much weaker than the high affinity ligands mentioned above (**Fig. 5A and L**). In contrast, LRP1 binding to progranulin or fibulin-1C was not observed at all (**Fig. 5F and I**). We confirmed that cathepsin D directly binds to immobilised sLRP1 ($K_{D,app}$ >500 nM) but negligible binding was observed for sLRP1-II (**Suppl Fig. 6**). These results indicate that the molecules co-isolated with sLRP1-II include not only direct LRP1 binders but also non LRP1 binders that may interact with LRP1 indirectly, possibly *via* true ligands.

LRP1-dependent clearance of novel LRP1 ligands in mouse embryonic fibroblasts

Newly identified proteins that directly bind to LRP1 were tested for their endocytic clearance by cells *via* LRP1 using wild-type (WT) mouse embryonic fibroblasts (MEFs) and LRP1-deficient MEFs [43] to confirm if the endocytic pathway is LRP1-dependent. Recombinant HGFA, HMGB2, CEMIP, SLIT2, ADAMTS1, TSG6, IGFBP7 and SPARC (each 10 nM) were incubated with the cells for 8 h and these molecules in conditioned medium and cell lysate were detected by Western blot analysis using anti-FLAG or His tag antibody. The amounts of exogenously added HMGB2, CEMIP, SLIT2, ADAMTS1, TSG6 and IGFBP7 in the conditioned medium were reduced in WT MEFs by 59%, 92%, 65%, 62%, 80% and 45%, respectively, compared to LRP1-deficient MEFs, whereas no changes were observed for HGFA (**Fig. 6A–G**). SPARC was also reduced in WT MEFs by 25% compared to LRP1-deficient cells but the differences appeared to be not statistically significant (**Fig. 6H**). Exogenously added SLIT2, ADAMTS1, TSG6 and IGFBP7 were also detected in the cell lysate and the slightly lower amounts of SLIT2, TSG6 and IGFBP7 were detected in WT compared to LRP1-deficient MEFs (**Fig. 6D–G**). These results indicate that if the same concentration of LRP1 ligands is present in the extracellular milieu, the ligands with higher affinity are internalized *via* LRP1-mediated endocytosis more rapidly than low affinity binders (**Fig. 6I and Table 4**).

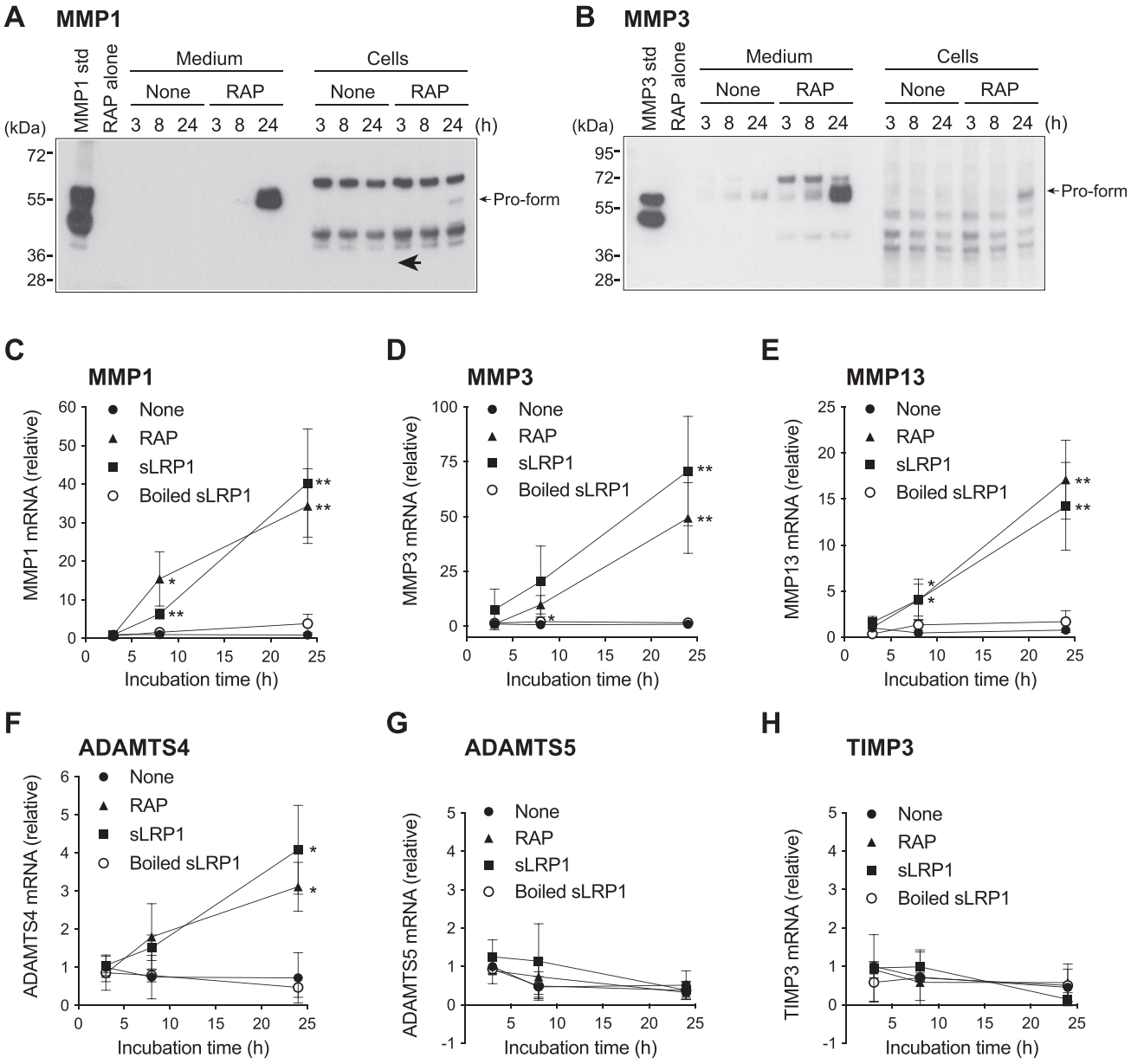


Fig. 3. Inhibition of LRP1-mediated endocytosis induces transcriptional modulation.
Human normal chondrocytes from three different donors (M1, M3 and F1) were incubated with serum-free DMEM containing CT1746 (100 μM) and the protease inhibitor cocktail (1/500) in the absence or presence of 200 nM RAP (*A and B*), 10 nM sLRP1 or boiled and denatured sLRP1 (*C-H*) for 0−24 h. Representative Western blotting analysis of MMP1 (*A*) and MMP3 (*B*) in the media and cell lysate detected using the anti-MMP1 and anti-MMP3 antibodies. TaqMan real-time PCR showing relative levels of mRNA for MMP1 (*C*), MMP3 (*D*), MMP13 (*E*), ADAMTS4 (*F*), ADAMTS5 (*G*) and TIMP3 (*H*) in human chondrocytes. Points represent the means ± *SD*. *, $p < 0.05$, **, $p < 0.01$, by 2-tailed Student's t test. *Std*: 10 nM purified protein for pro- and activated forms of MMP1 and MMP3.

LRP1-mediated endocytosis regulates extracellular availability of CEMIP, SLIT2, HMGB2, ADAMTS1 and TSG6 in human chondrocytes

After confirming that the endocytic pathway of the novel LRP1 ligands is LRP1-dependent, we investigated if this regulation also occurs in human chondrocytes. Western blot analysis showed that endogenously produced CEMIP and HMGB2 were rarely detectable in the conditioned medium of human chondrocytes after 24-h incubation without sLRP1-II but markedly increased in the presence of 5 nM sLRP1-II (**Fig. 7A and B**). The sLRP1-II

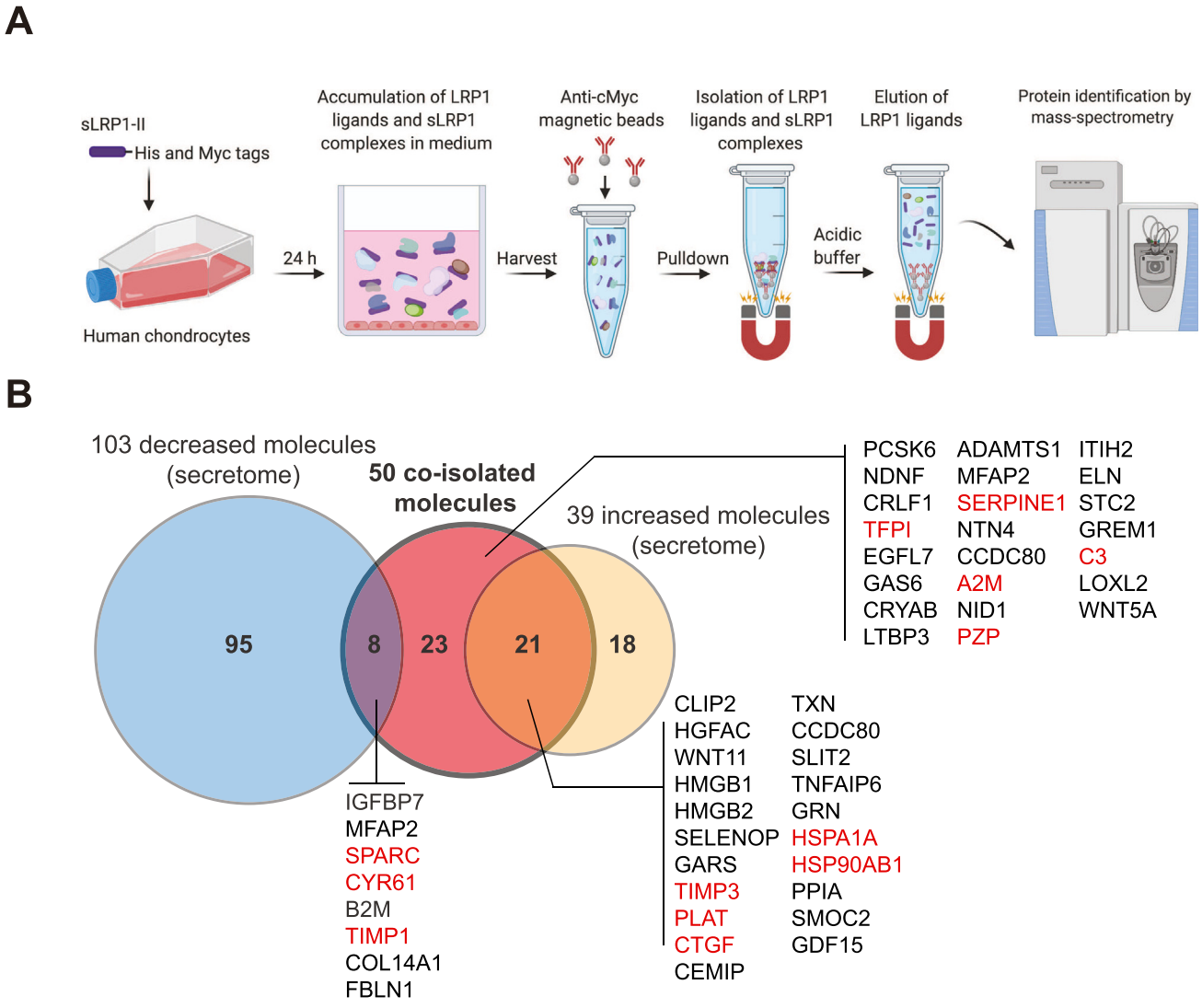


Fig. 4. Chondrocyte LRP1 interactome consists of a variety of novel ligand candidates.
A, Workflow of isolation and identification of LRP1 ligands in human chondrocytes from four different donors (M1, M2, F1 and F2). Briefly, human chondrocytes were incubated with of serum-free DMEM containing CT1746 (100 μM) and the protease inhibitor cocktail in the absence (control) or presence of 5 nM sLRP1-II for 24 h. The conditioned medium was collected and further incubated with anti-c-Myc paramagnetic Dynabeads at 4°C for 1 h. sLRP1-II and the magnetic beads complexes were then isolated using the magnetic stand, washed and eluted with 0.1 M glycine buffer (pH 3.0) for 10 min at 4°C. The workflow was created with BioRender (https://biorender.com). *B*, Venn diagrams showing secreted proteins that were co-isolated with sLRP1-II (red)(the proteins identified in all 4 biological replicates of sLRP1-II-treated cells, but only in 0-1 replicates of untreated control cells, and the proteins >2.5 fold increased in sLRP1-II treated cells compared to the control cells, FDR <0.01), secreted proteins increased (orange) or decreased (blue)(FDR <0.01) in the medium of chondrocytes treated with sLRP1-II (Fig. 2). Gene name for previously reported LRP1 ligands is highlighted in red (For interpretation of the references to color in this figure legend, the reader is referred to the web version of this article.).

treatment increased the levels of SLIT2, ADAMTS1 and TSG6 in the medium of chondrocytes approx. 10-, 2.5- and 2.8-fold, respectively, compared to the control (Fig. 7C–E), whereas no significant changes were observed for IGFBP7 (Fig. 7F). Immunofluorescent confocal microscopy analysis further revealed that punctate staining of CEMIP, HMGB2, SLIT2 and ADAMTS1 was detected within the cells, and some of the staining colocalized with early endosome antigen 1 (EEA1), a marker for early endosomes (Fig. 7G–J). The fluorescent signal of these ligands was absent in cells incubated without the ligands, indicating the specificity of the staining. The intracellular fluorescent signal for these ligands

Table 3. Secreted molecules co-immunoprecipitated with sLRP1-II from medium of human chondrocytes.

Description	Gene name	Accession	Ratio (sLRP1-II vs control)	p-value
Proteins identified only with sLRP1-II				
Cartilage intermediate layer protein 2	CILP2	Q8IUL8		
Hepatocyte growth factor activator	HGFAC	Q04756		
Protein Wnt-11	WNT11	O96014		
High mobility group protein B1	HMGB1	P09429		
Proprotein convertase subtilisin/kexin type 6	PCSK6	P29122		
High mobility group protein B2	HMGB2	P26583		
Selenoprotein P	SELENOP	P49908		
Protein NDNF	NDNF	Q8TB73		
Cytokine receptor-like factor 1	CRLF1	O75462		
*Tissue factor pathway inhibitor	TFPI	P10646		
Epidermal growth factor-like protein 7	EGFL7	Q9UHF1		
Growth arrest-specific protein 6	GAS6	Q14393		
Alpha-crystallin B chain	CRYAB	P02511		
Latent-transforming growth factor beta-binding protein 3	LTBP3	Q9NS15		
Glycine−tRNA ligase	GARS	P41250		
Proteins >2.5 fold increased with sLRP1-II				
*Metalloproteinase inhibitor 3	TIMP3	P35625	1301.54	7.16E-06
*Tissue-type plasminogen activator	PLAT	P00750	457.60	1.84E-08
Insulin-like growth factor-binding protein 7	IGFBP7	Q16270	293.50	1.04E-06
*Connective tissue growth factor	CTGF	P29279	292.52	7.76E-06
Cell migration-inducing and hyaluronan-binding protein	CEMIP	Q8WUJ3	236.61	9.10E-08
A disintegrin and metalloproteinase with thrombospondin motifs 1	ADAMTS1	Q9UHI8	220.73	4.48E-08
Microfibrillar-associated protein 2	MFAP2	P55001	174.38	1.09E-06
*SPARC	SPARC	P09486	96.43	5.76E-07
*Plasminogen activator inhibitor 1	SERPINE1	P05121	69.21	5.77E-07
*Protein CYR61	CYR61	O00622	59.25	6.92E-04
Netrin-4	NTN4	Q9HB63	58.71	3.60E-06
Thioredoxin	TXN	P10599	53.13	1.96E-05
Coiled-coil domain-containing protein 80	CCDC80	Q76M96	34.00	4.86E-03
Slit homolog 2 protein	SLIT2	O94813	27.11	9.80E-08
*Alpha-2-macroglobulin	A2M	P01023	22.02	5.28E-06
Tumor necrosis factor-inducible gene 6 protein	TNFAIP6	P98066	16.24	1.22E-03
Beta-2-microglobulin	B2M	P61769	12.49	1.32E-02
Nidogen-1	NID1	P14543	11.30	2.23E-03
*Pregnancy zone protein	PZP	P20742	11.00	2.35E-06
*Metalloproteinase inhibitor 1	TIMP1	P01033	9.51	1.47E-03
Inter-alpha-trypsin inhibitor heavy chain H2	ITIH2	P19823	9.20	6.03E-03
Elastin	ELN	P15502	8.28	3.55E-02
Progranulin	GRN	P28799	8.24	3.41E-05
*Heat shock 70 kDa protein 1A	HSPA1A	P0DMV8	8.01	3.06E-06
Collagen alpha-1(XIV) chain	COL14A1	Q05707	7.56	1.09E-03
*Heat shock protein HSP 90-beta	HSP90AB1	P08238	6.64	4.41E-06
Stanniocalcin-2	STC2	O76061	6.05	5.65E-05
Fibulin-1	FBLN1	P23142	5.25	3.37E-03
Gremlin-1	GREM1	O60565	5.12	1.10E-02
Peptidyl-prolyl cis-trans isomerase A	PPIA	P62937	4.55	1.43E-03
SPARC-related modular calcium-binding protein 2	SMOC2	Q9H3U7	4.03	7.43E-03
*Complement C3	C3	P01024	3.89	1.30E-04
Growth/differentiation factor 15	GDF15	Q99988	2.79	7.70E-03
Lysyl oxidase homolog 2	LOXL2	Q9Y4K0	2.79	4.64E-04
Protein Wnt-5a	WNT5A	P41221	2.73	3.08E-02

All proteins >2.5 fold increased with sLRP1-II are FDR <0.01.

*LRP1 ligands already reported.

Molecules significantly (FDR <0.01) increased with sLRP1-II in the secretome analysis

was markedly reduced in the presence of RAP or sLRP1, suggesting that their internalization was mediated by LRP1.

High-affinity LRP1 ligands are tightly regulated by LRP1 in knee articular cartilage tissue *in vivo*

Given the complexity of extracellular environment and the possible competition between LRP1 and sulphated glycosaminoglycans (GAGs) in articular cartilage [44,45], we investigated newly identified high-affinity LRP1 ligands SLIT2 and CEMIP in knee articular cartilage of LRP1 conditional KO mice. Due to the early embryonic lethality of *LRP1* deletion [6], we have established a transgenic mouse line harbouring floxed LRP1 and the ROSA26$^{(cre/ERT2)}$ promoter (*LRP1*$^{(flox/flox)}$/*ROSA26*$^{(cre/ERT2)}$)(**Fig. 8A**). The control (LRP1$^{flox/flox}$) and homozygote (LRP1$^{flox/}$

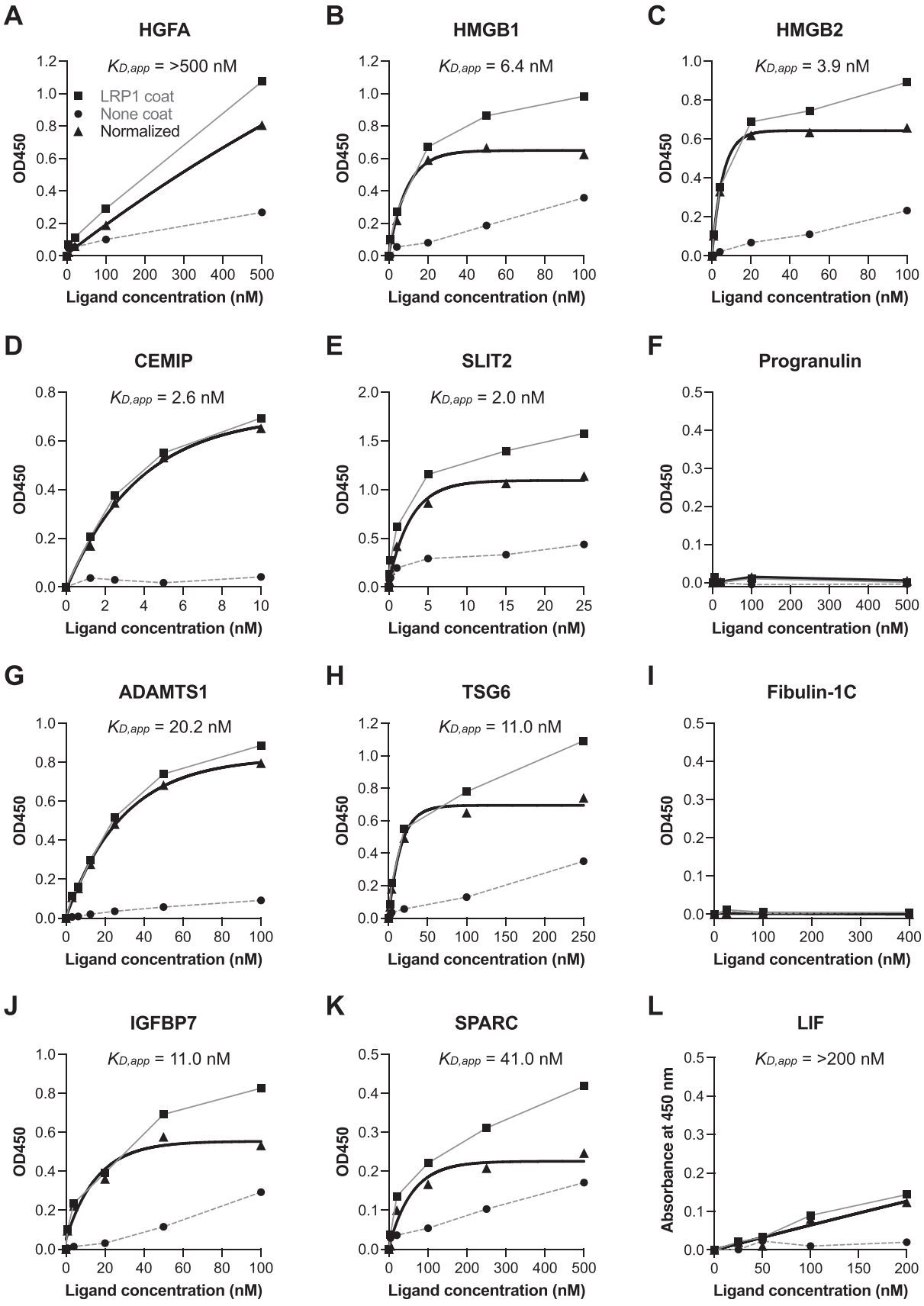


Fig. 5. Newly identified LRP1 ligands exhibit a wide range of affinities.

^{flox}Rosa$^{Cre/ERT2}$) conditional LRP1 KO mice were given tamoxifen by intraperitoneal (IP) injection and knee joint tissues were collected 3 days after the third dose of tamoxifen. qPCR analysis of total RNA extracted from the mouse skin tissue showed >79% reduction of *Lrp1* mRNA in the KO compared to wild-type tissue (**Fig. 8B**). Histological investigation of LRP1 in knee joint tissue revealed that LRP1 is abundantly expressed in the cell membrane of chondrocytes at the superficial area of cartilage and of the cells in the medial meniscus, however these immunosignals were markedly diminished in the KO mice (**Fig. 8C**). SLIT2 and CEMIP were detected in some chondrocytes in the control whereas stronger immunosignal of these ligands was observed in LRP1 KO tissue (**Fig. 8D**). Like SLIT2 and CEMIP, connective tissue growth factor (CTGF), an important LRP1 ligand [46,47], showed a negative correlation between absence of LRP1 and its abundance in cartilage *in vivo*.

Discussion

This study found that inhibition of LRP1-mediated endocytosis in human chondrocytes results in cell death, alteration of the entire secretome and transcriptional modulation. Our systematic approach revealed the specificity and the extent of the chondrocyte LRP1 ligandome that illustrates novel biological roles of LRP1 in cartilage and potentially other tissues, and the pathological conditions when LRP1 ligands are present in the tissue for extended periods.

We showed that both sLRP1, which acts as a soluble decoy receptor and competes with endogenously expressed LRP1, and RAP, which binds to LRP1 and competes with endogenous ligand binding, induce chondrocyte cell detachment and death (**Fig. 1**). Modulation of cell adhesion by inhibition of LRP1 and ligand interaction is not surprising as LRP1 is known to regulate focal adhesion number, composition and turnover [48–50]. Furthermore, it interacts with β1 integrin thus regulating its function [48,51]. Previous studies have indicated a role of LRP1 in cell survival and death [52–54]. In agreement with these studies, we found pro-cell survival role of LRP1 in human articular chondrocytes. Furthermore, several studies demonstrated cell survival and death functions for both previously reported and newly identified LRP1 ligands such as TIMP3 [55–60], ADAMTS5 [61], CTGF [62,63], CEMIP [64], SLIT2 [65,66], IGFBP7 [67–69] and HMGB2 [70]. The mechanisms by which LRP1 ligands regulate cell survival in chondrocytes remain unclear but the prolonged presence of one or several LRP1 ligands in the extracellular milieu may gradually alter cellular environment and metabolism leading to cell death.

The chondrocyte secretome analysis revealed a huge impact of LRP1 blockade with significant changes in 448 molecules including 320 intracellular, 17 transmembrane, and 142 secreted proteins. The proteomics methods used in this study were highly sensitive, allowing for the detection of intracellular proteins secreted by unconventionally means [71] and/or few blasted cells or extracellular vesicles. Although 5 nM sLRP1-II did not induce significant chondrocyte cell death up to 24 h incubation, it is possible that intracellular proteins from a small population of blasted cells contributed to the observed differences. Furthermore, given transcriptional modulations caused by inhibition of LRP1 and ligand interaction, sLRP1-II treatment may affect expression of intracellular proteins. On the other hand, our previous study showed that RAP treatment inhibits activity of ADAM10 and alters release of several transmembrane proteins in HEK293 cells [41]. This is potentially due to reduced activity of ADAM10 caused by accumulation of its inhibitor TIMP3. Accumulation of LRP1 ligands alter release of transmembrane proteins in human chondrocytes possibly through modulation of proteolytic activity of membrane-bound proteolytic enzymes called sheddase (s).

Importantly, LRP1 ligands can affect each other, as well as molecules that do not interact with LRP1, in several ways including transcriptional modulation, complex formation, modulation of activity and localization, and proteolytic degradation. It has been reported that RAP increases mRNA levels of pro-inflammatory mediators such as TNFα, interleukin-6 and C–C motif chemokine ligand 2 in macrophages [36]. Considering functional diversity of LRP1 ligands, transcriptional modulation of several molecules shown in this study could be the tip of the iceberg. Cathepsin D directly binds to LRP1 β-chain [42] but not to sLRP1-II (**Suppl Fig. 6**). Our secretome analysis showed that the sLRP1-II treatment increased cathepsin D in the medium of

Full-length sLRP1 was coated onto microtiter plates and the binding of various concentrations of HGFA (*A*), HMGB1 (*B*), HMGB2 (*C*), CEMIP (*D*), SLIT2 (*E*), progranulin (*F*), ADAMTS1 (*G*), TSG6 (*H*), fibulin-1C (*I*), IGFBP7 (*J*), SPARC (*K*) and LIF (*L*) was measured using anti-FLAG M2 or anti-His tag antibody and a horseradish peroxidase-conjugate secondary antibody as described under "Experimental procedures". Mean values of technical duplicates for none-coating, LRP1-coating and after normalization by subtracting the none-coating values from the LRP1-coating values were shown as circles, squares and triangles, respectively. Extrapolated $K_{D,app}$ values were estimated based on one-phase decay nonlinear fit analysis (black lines).

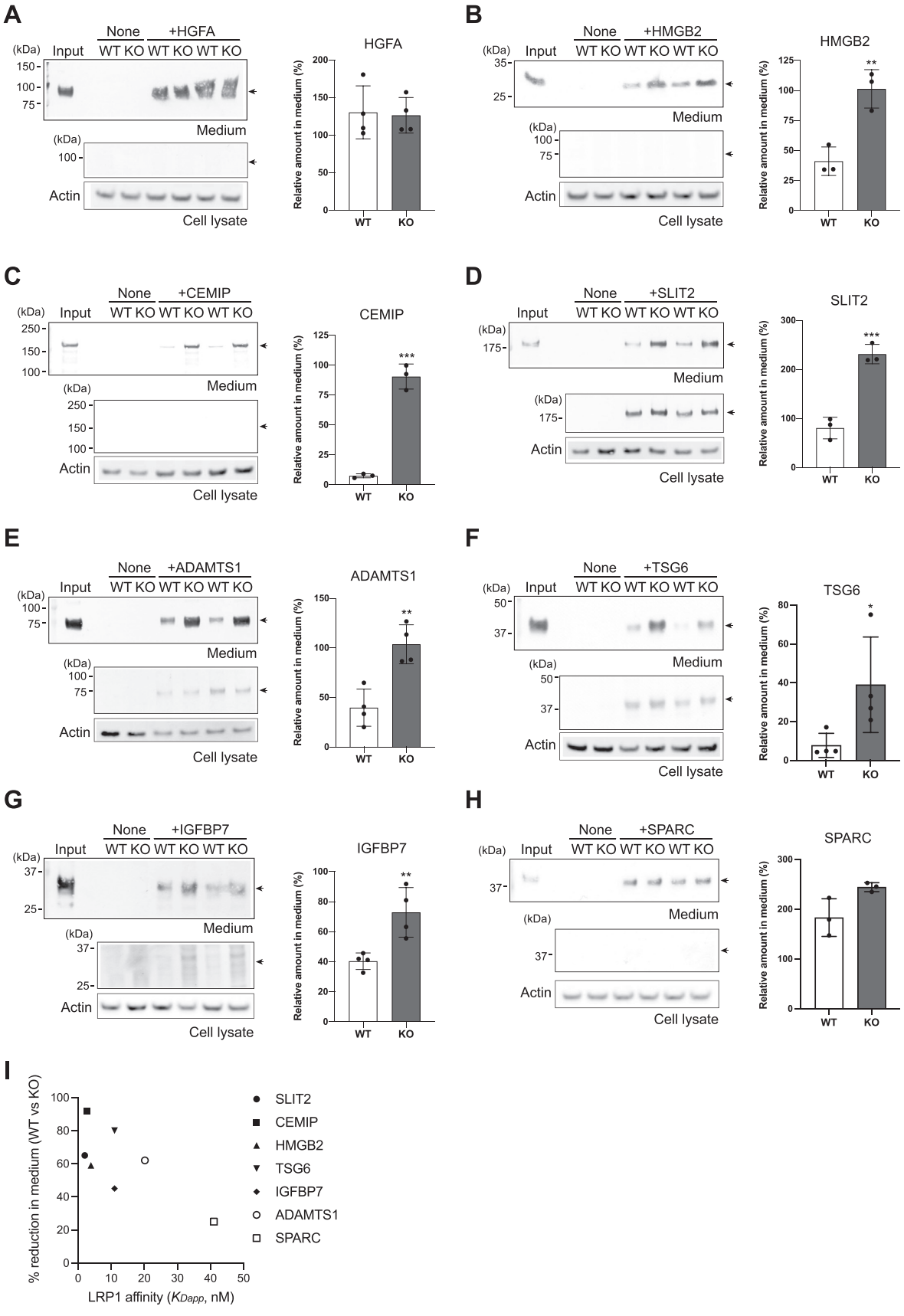


Fig. 6. LRP1-dependent clearance of novel LRP1 ligands in mouse embryonic fibroblasts

chondrocytes (**Fig. 2**), suggesting that extracellular availability of cathepsin D is regulated by both LRP1 and LRP1 ligands. Negligible binding of progranulin and fibulin-1C to LRP1 suggests that these molecules indirectly interact with LRP1 *via* LRP1 ligands (**Fig. 5**). It has been reported that prosaposin, one of previously reported LRP1 ligands, interacts with progranulin and regulates its levels *in vitro* and *in vivo* [72,73]. It has also been reported that fibulin-1C binds to newly identified LRP1 ligands, ADAMTS1 [74] and CTGF [75]. To date, several extracellular proteolytic enzymes, which cleave a broad range of substrates, have been identified as LRP1 ligands [4,5,45]. Proteolytic degradation by LRP1 ligands is thus likely to contribute to reduction of the number of secreted proteins in particular ECM molecules. Indeed, levels of versican, nidogen-2 and biglycan, all previously reported substrates for ADAMTS1 [76−78], were reduced in the medium of chondrocytes treated with sLRP1-II (**Table 2**).

The correlation between the affinity of LRP1 and the rate of endocytosis was previously demonstrated for ADAMTS4 and 5 isoforms [21]. The data presented here also supported this notion for various LRP1 ligands. Importantly, several LRP1 ligands bind to both LRP1 and sulphated GAGs, with their extracellular availability determined by their relative affinity for each [44,45,79]. It should be noted that neither ADAMTS4 and 5, nor MMP13 were identified in the conditioned medium of chondrocytes either in the absence or presence of sLRP1-II by our proteomics analysis. These results suggest the possibility that the majority of these enzymes were anchored to the ECM or cell surface *via* sulphated GAGs when LRP1-mediated endocytosis was blocked. The extracellular environment in articular cartilage is a complex matrix where chondrocytes are surrounded by a thin layer of pericellular ECM followed by an abundant ECM mainly consisting of aggrecan proteoglycan and type II collagen fibrils. Nonetheless, markedly increased SLIT2, CEMIP and CTGF in knee articular cartilage from conditional LRP1 knockout mice (**Fig. 7**), indicate that LRP1 is a master regulator of extracellular availability of high-affinity ligands in the tissue *in vivo*.

Our Western blot analysis showed that MMP1 and MMP3 were markedly increased in medium of RAP- or sLRP1-treated chondrocytes (**Fig. 3**). In contrast, both MMPs were not significantly increased by sLRP1-II treatment in the secretome analysis (**Fig. 2** and **Suppl Table 1**). This is potentially due to technical limitations of our proteomics method. Label-free quantitative proteomics relies on the quantification of a limited number of unique peptides, that are not representative of the full protein. There may be fragments of MMP1 and MMP3 that were not detected by our Western blot analysis but generate peptides that are quantified by mass spectrometry. It is also possible that peptides arisen from tryptic digestion of these proteinases may have the same retention time of other peptides arisen from much more abundant protein(s). In this case, MMP1 and MMP3 signals will be covered and unidentified. The controversial results of abundance of these proteinases in mass-spec and Western blot analysis emphasize the need of validating proteomics data by using different methods. These and other technical limitations may also be a possible reason to explain why ADAMTS4 and 5, and MMP13 were not identified by the proteomics analysis.

This study generated new information about the pathobiological functions of the key molecules that are regulated by LRP1-mediated endocytosis and their connection to the development of OA. Extracellular HMGB molecules function as alarmins, which are endogenous molecules released upon tissue damage to activate the immune system. HMGB2 KO mice exhibit earlier onset of OA and a more severe progression, which is associated with a profound reduction in cartilage cellularity [70]. By contrast, HMGB1 acts as a late mediator of inflammation and contributes to prolonged and sustained systemic inflammation in subjects with rheumatoid arthritis (see [80] for review). Importantly, hyaluronan degradation is highly associated with the risk of OA progression [81,82]. CEMIP functions as a hyaluronan depolymerase [83] and is highly relevant to OA pathogenesis [84−86]. Momoeda et al recently demonstrated that cartilage destruction and osteophyte formation are suppressed in CEMIP deficient mice [87], suggesting a role of CEMIP in the progression of OA. Expression levels of CEMIP and CTGF are correlated with disease severity in OA patients [88−90], and we found that their levels are

Wild-type (WT) and LRP1 deficient (KO) MEFs (n = 3 or 4 each for *A, D, F* and *H*, or *B, C, E* and *G*, respectively) were cultured for 8 h in the absence (None) or presence of either 20 nM HGFA (*A*), HMGB2 (*B*), CEMIP (*C*), SLIT2 (*D*), ADAMTS1 (*E*), TSG6 (*F*), IGFBP7 (*G*) or SPARC (*H*) for 8 h. Representative Western blotting analysis of these proteins in the media and cell lysate detected using the anti-His tag antibody (*A, C, D, E, G* and *H*) or anti-FLAG M2 antibody (*B* and *F*)(*left panels*). Beta-actin in the cell lysate was detected by Western blotting using an anti-actin antibody. Band intensity was quantified by densitometry and the amount of each protein was expressed as a percentage of the amount of each protein at 0 h (Input), which was taken as 100% (*right panels*). Circles represent a replicate and bars show the mean ± *SD*. *, $p < 0.05$, **, $p < 0.01$, ***, $p < 0.001$ by 2-tailed Student's t test.

p values were evaluated by 2-tailed Student's t test. *I,* The estimated affinity of SLIT2, CEMIP, HMGB2, TSG6, IGFBP7, ADAMTS1 and SPARC for LRP1 ($K_{D,app}$) was plotted against the percentage reduction of their amounts in the conditioned medium of WT compared to LRP1 KO MEFs.

Table 4.

	$K_{D,app}$ values for LRP1 binding (nM)	Exogenous ligands in MEFs medium (% *vs* LRP1 KO MEFs)	Endogenous levels in chondrocyte medium with sLRP1-II (fold change *vs* control)	
			Secretome	Western blotting
SLIT2	2.0	↓ 65***	↑ 212.8****	↑ 2.5
CEMIP	2.6	↓ 92***	↑ 42.2****	↑ >15681
HMGB2	3.9	↓ 59**	↑ 19.4*	↑ >25.1
HMGB1	6.4	ND	↑ 3.9**	ND
TSG6	11.0	↓ 80*	↑ 1.7*	↑ 2.8
IGFBP7	11.0	↓ 45**	↓ 3.5****	NS
ADAMTS1	20.2	↓ 62**	ND	↑ 10
SPARC	41.0	NS	↓ 5.2***	ND
LIF	>200	ND	↑ 12.4***	ND
HGFA	>500	NS	↑ 26.6***	ND
Progranulin	No binding	ND	↑ 13.6****	ND
Fibulin-1	No binding	ND	↓ 8.4****	ND

Extrapolated $K_{D,app}$ values (nM), the percentage changes of the amount of exogenously added ligands in the medium of WT compared to LRP1 KO MEFs, and the fold changes of the amount of endogensouly produced ligands in medium of chondrocytes treated with sLRP1-II compared to the control detected by sectetome or Western blot analysis were estimated based on the results in Fig 5, Fig 6, Fig 2 and Fig 7, respectively. *$p < 0.05$, **$p < 0.01$, ***$p < 0.001$, ****$p < 0.0001$ by 2-tailed Student's t test. *ND*: Not determined, *NS*: Not statistically significant.

increased in cartilage from LRP1 KO mice *in vivo* (**Fig. 7**). Notably, hyaluronan is endocytosed *via* clathrin-coated pits and degraded in vesicles in HEK293 cells overexpressing CEMIP [91]. LRP1 not only regulates extracellular availability of CEMIP but may also play a role in transporting both CEMIP and hyaluronan to the coated pits where hyaluronan is degraded. TSG6 also binds to hyaluronan [92] and its protein and mRNA levels are increased in OA cartilage [93,94]. In the presence of inter-α-inhibitor (IαI), which was identified as a LRP1 ligand candidate (**Table 3**), TSG6 catalyzes the formation of an anti-inflammatory stabilised hyaluronan-aggrecan assembly [95–97]. However, TSG6 blocks hyaluronan-aggrecan assembly in the absence of IαI [98]. Furthermore, our previous study demonstrated that IαI is proteolytically cleaved by ADAMTS5, MMP3, MMP7 and MMP13 [99]. Considering that CEMIP, TSG6, ADAMTS5 and MMP13 are all regulated by LRP1, increased LRP1 shedding in OA effectively leads to cartilage destruction by both increasing extracellular activity of cartilage-degrading proteinases [19] and destabilizing cartilage ECM assembly.

Accumulating evidence suggests a role of LRP1 in the regulation of Wnt signalling, which governs a myriad of biological processes underlying the development and maintenance of adult tissue homeostasis. Macrophage LRP1 increases Wnt/β-catenin pathway by directly binding to and effectively removing secreted frizzled-related protein 5, which prevents Wnt binding to its receptor [100]. LRP1 also stimulates Wnt/β-catenin pathway and prevents intracellular cholesterol accumulation in fibroblasts [101]. A recent study also demonstrated that LRP1 regulates expression of Wnt family member 4 in chondrocytes through transforming growth factor-β1 signalling in chondrocytes [102]. On the other hand, it has been reported that LRP1 interacts with Frizzled1 and downregulates Wnt/β-catenin pathway in HEK293T cells [103]. Newly identified LRP1 ligands in this study are also involved in the Wnt pathway. For example, HMGB2 enhances the binding of lymphoid enhancer-binding factor 1 (Lef-1), a crucial transcription factor for Wnt/β-catenin pathway, to its target sequence and potentiates transcriptional activation of the Lef-1-β-catenin complex [104]. The HMG domain within HMGB2 is crucial for interaction with Lef-1, suggesting that both HMGB2 and HMGB1 may be involved in this function. CEMIP also enhances Wnt/β-catenin signalling and bone formation of osteoblastic stem cells [105]. Moreover, we have identified WNT5a and WNT11 as LRP1 ligand candidates (**Table 3**). These studies emphasise a role of LRP1 in the Wnt pathway and we are currently investigating how the interaction between LRP1 and these WNTs affects Wnt signalling pathways.

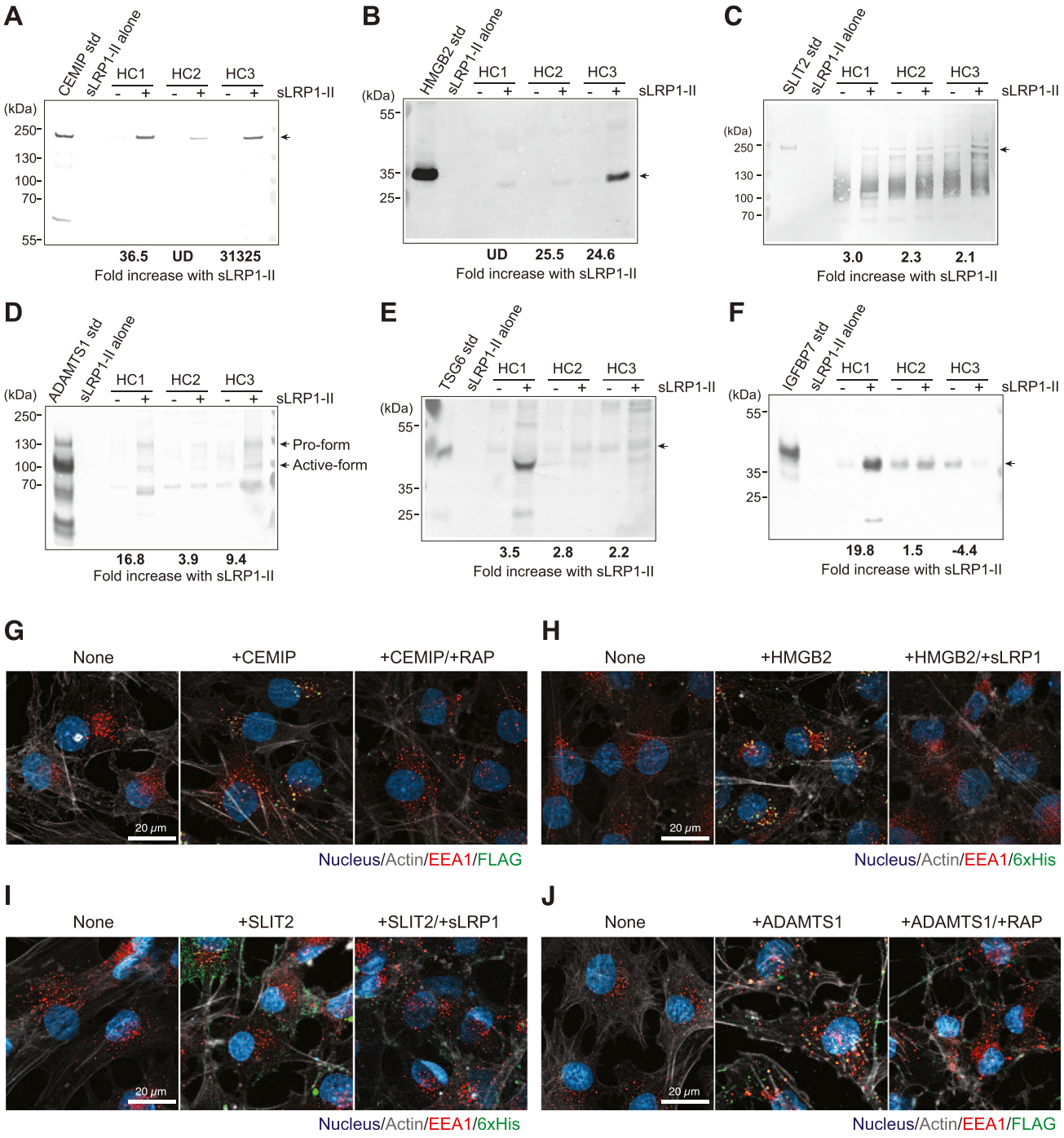


Fig. 7. LRP1-mediated endocytosis regulates extracellular availability of CEMIP, HMGB2, SLIT2, ADAMTS1 and TSG6 in human chondrocytes.

A-F, Human normal chondrocytes from three different donors (M1, F1 and F2) were incubated with serum-free DMEM containing CT1746 (100 μM) and the protease inhibitor cocktail (1/500) in the absence or presence of 5 nM sLRP1-II for 24 h. The conditioned medium was collected and then subjected to Western blot analysis using anti-CEMIP (*A*), HMGB2 (*B*), SLIT2 (*C*), ADAMTS1 (*D*), TSG6 (*E*) and IGFBP7 (*F*) antibodies. Band intensity was quantified by densitometry and the fold increase in the presence of sLRP1-II compared to the absence of sLRP1-II in each patient shown under the blot image. *UD*: The fold difference undetermined due to the lack of the protein band in the absence of sLRP1-II. *Std*: 5 nM purified protein of CEMIP and 20 nM purified proteins of HMGB2, SLIT2, ADAMTS1, TSG6 and IGFBP7. *G-J*, Presentative confocal microscopy images for internalization of CEMIP (*G*), HMGB2 (*H*), SLIT2 (*I*) and ADAMTS1 (*J*) by human chondrocytes. Cells (M1 and F1) were incubated with 10 nM CEMIP or 20 nM HMGB2, SLIT2 or ADAMTS1 in the presence or absence of 500 nM RAP or 40 nM sLRP1 for 1 h. Internalized ligands, EEA1, cytoskeleton, and nucleus were visualized as described under “Experimental procedures”. Scale bar, 20 μm.

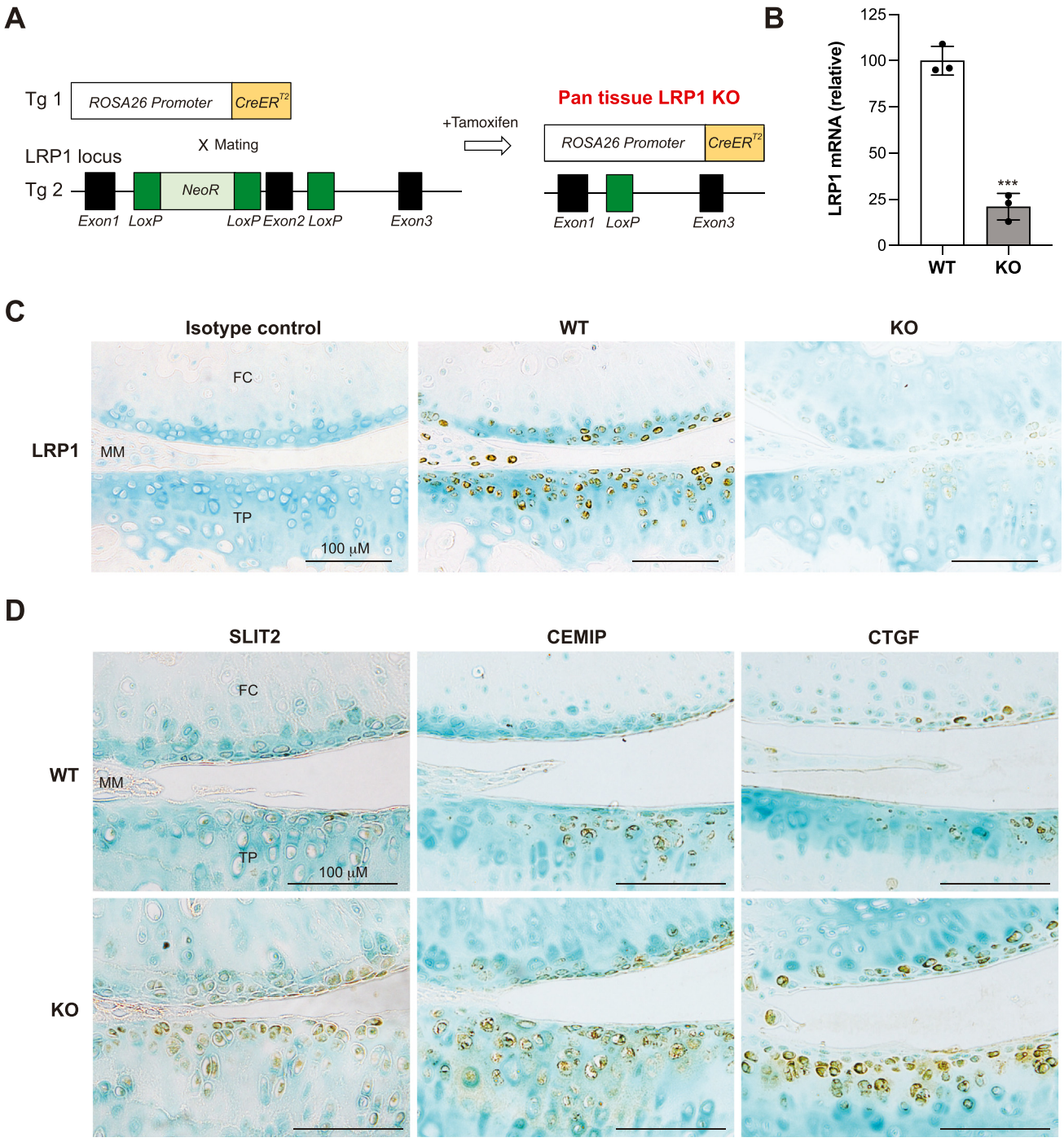


Fig. 8. High-affinity LRP1 ligands are tightly regulated by LRP1 in knee articular cartilage tissue *in vivo*.
A, Schematic diagram showing the constructs used to generate pan-tissue LRP1 conditional knockout mice. Transgenic mouse lines harbouring ROSA26$^{(cre/ERT2)}$ promoter (Tg 1) and floxed *LRP1* (Tg 2) were used to establish a pan-tissue LRP1 conditional KO mice (*LRP1*$^{(flox/flox)}$/*ROSA26*$^{(cre/ERT2)}$). Tamoxifen activates *CreER*^{T2}, which translocates into nucleus to excise *LRP1* gene. *B-D, LRP1*$^{(flox/flox)}$/*ROSA26*$^{(cre/ERT2)}$(KO) and *LRP1*$^{(flox/flox)}$ (WT) mice (n = 3 each) were administrated by IP injections for three times over a week with 2 and 4 days interval. The mice were culled 3 days after the final dose of tamoxifen. *B*, TaqMan real-time PCR showing relative levels of mRNA for LRP1 in the skin tissue. Circles represent individual cartilage donors and bars show the mean ± *SD*. ***, p = 0.0002 by 2-tailed Student's t test. *C and D*, Representative immunohistochemical staining images of LRP1 (*C*), SLIT2, CEMIP and CTGF (*D*) in knee articular cartilage. Scale bar, 100 μm. *FC*, femoral condyle. *MM*, medial meniscus. *TP*, tibial plateau.

This study provided important information about possible roles of LRP1 in other tissue contexts and diseases. SLIT2 binds to Roundabout 1 and 2 receptors [106] and plays a crucial role in neuronal outgrowth in embryogenesis [107,108]. HGFA, which directly binds to LRP1 and was increased in the medium of chondrocytes by sLRP1-II treatment, is a serine protease responsible for converting HGF into the active two-chain form [109–111]. HGF is considered to play a major role in the repair and regeneration of various tissues, including the liver, kidney, lung, and stomach [112]. Notably, both HGF activation and tissue regeneration were markedly impaired in injured intestinal tissue of HGFA-deficient mice [110,111], indicating the important function of HGFA during tissue repair process. Although HGFA is the major HGF activator, previously reported LRP1 ligands including urokinase-type plasminogen activator, tissue plasminogen activator and coagulation factor XI were also able to activate HGF *in vitro* [113,114]. Another newly identified LRP1 ligand, ADAMTS1, is broadly expressed and essential for normal growth, structure, and function of the kidney, adrenal gland, female reproductive-organ, and myocardial trabeculation during heart development (see [115] for review), and limb joint development [116]. Interestingly, recent studies revealed emerging roles of CEMIP in bone development [105,117], inflammation and anti-microbial activity [118]. A study using CEMIP-deficient mice revealed that hyaluronan metabolism by CEMIP is involved in endochondral ossification during postnatal development by modulation of angiogenesis and osteoclast recruitment at the chondro-osseous junction [117]. In another study, CEMIP-deficient mice showed no hyaluronan digestion and significantly less evidence of skin infection after an intradermal bacterial challenge by *Staphylococcus aureus* [118]. This information about the physiological functions of newly identified ligands implies LRP1 in organ morphogenesis, tissue regeneration and infection.

The methodology established in this study could be useful for other tissue contexts and diseases. One of the limitations of such an approach is that several LRP1 ligands were discovered with conflicting functions. For example, both proteases and their specific inhibitors were identified as LRP1 ligands. It is thus difficult to predict any net outcome of LRP1-mediated endocytosis and its dysregulation from the results of this study. However, our elucidation of a cartilage-specific ligandome opens potential new avenues of therapeutic intervention in diseases characterized by dysregulated LRP1-mediated endocytosis. By designing agents able to modulate the endocytosis of cartilage specific LRP1 ligands, it will be possible to counteract the negative effects of LRP1 dysregulation. For example, variants of TIMP3 resistant to LRP1-mediated endocytosis [119] and soluble LRP1 subcluster that selectively block TIMP3 endocytosis [35] have already been engineered to contrast excessive ADAMTS5 activity. Combination of functional studies using cells or animal models and more complete tissue specific LRP1 ligandome identification is required for better understanding of the physiological functions of LRP1, and the detrimental effects of its dysregulation.

Experimental procedures

Reagents and antibodies

The sources of materials used were as follows: Pierce™ Anti-c-Myc magnetic beads, RNase Inhibitor, 4–12% Bis-Tris NuPage Gels and fetal bovine serum (FBS) from Thermo Fisher Scientific (Waltham, MA); purified human full-length LRP1 from BioMac (Leipzig, Germany); recombinant human progranulin (C-terminal His tag, 2420-PG), SLIT2 (C-terminal His tag, 8616-SL), HGFA (C-terminal His tag, 1514-SE), TSG6 (C-terminal His tag, 2104-TS), anti-His tag mouse monoclonal antibody (MAB050) and the basic-based antigen unmasking solution (CTS013) from R&D Systems (Minneapolis, MN); anti-FLAG M2 mouse monoclonal antibody (F1804), protease Inhibitor cocktail consisting of aprotinin, bestatin, E-64, leupeptin and pepstatin A (P1860), tamoxifen free base, corn oil, lysis buffer, REDtaq ReadyMix PCR reaction mix, DPX mounting media, Dulbecco's Modified Eagle's Medium/Nutrient Mixture F-12 Ham (DMEM/F12) and bovine serum albumin (BSA) from Sigma (Dorset, UK); recombinant human HMGB1 (C-terminal His tag, 10326-H08H), IGFBP7 (C-terminal His tag, 13100-H08H), SPARC (C-terminal His tag, 10929-H08H) and LIF (C-terminal His tag, 14890-H08H) from Sino Biological (Beijing, China); recombinant human HMGB2 (C-terminal His tag, TP720732) from ORIGENE (Rockville, MD); anti-rabbit alkaline phosphatase-linked antibody, anti-mouse alkaline phosphatase-linked antibody, anti-goat alkaline phosphatase-linked antibody and alkaline phosphatase substrate (5-bromo-4-choloro-3-indolyl 1-phosphate and nitroblue tetrazolium) from Promega (Southampton, UK); a hydroxamate-based MMP inhibitor CT-1746 (N1-[2-(S)-(3,3-dimethylbutanamidyl)]-N4-hydroxy-2-(R)-[3-(4-chlorophenyl)-propyl]-succinamide) from UCB Celltech (Slough, UK); anti-TSG6 rat monoclonal antibody (sc-65886), goat polyclonal anti-actin antibody (I-19) from Santa Cruz Biotechnology (Dallas, TX); anti-LRP1 β-chain rabbit monoclonal (ab92544), anti-CEMIP rabbit polyclonal (ab98947), anti-HMGB2 rabbit monoclonal (ab124670), anti-SLIT2 rabbit monoclonal (ab134166), anti-ADAMTS1 rabbit polyclonal (ab216977), anti-CTGF rabbit polyclonal (ab6992)

and anti-MMP1 mouse monoclonal (ab25483), anti-MMP3 mouse monoclonal (ab38907), and anti-IGFBP7 rabbit polyclonal (ab74169) antibodies from Abcam (Cambridge, UK); control rabbit IgG (I-1000-5), ImmPRESS peroxidase-micropolymer conjugated horse anti-rabbit IgG, Goat serum, Vectastain solution, methyl green, 3,3'-diaminobenzidine from Vector Laboratories (Burlingame, CA); anti-CEMIP rabbit polyclonal antibody (21129-1-AP) from Proteintech (Rosemont, IL); anti-ADAMTS1 mouse monoclonal antibody (TA804585) from ORIGENE (Rockville, MD). Recombinant human RAP [22], sLRP1-II [21], ADAMTS1 [76], ProMMP1 (E200A) [120], ProMMP3 (E202A) [120] were prepared as previously reported. All other reagents used were of the highest analytical grade available.

Isolation and culture of human articular chondrocytes

Healthy (normal) articular cartilage was obtained from the Stanmore BioBank, Institute of Orthopaedics, Royal National Orthopaedic Hospital, Stanmore from patients following informed consent and approval by the Royal Veterinary College Ethics and Welfare Committee (Institutional approval URN 2010 0004H). Articular cartilage was obtained from the femoral condyles of the knee following amputation due to soft tissue sarcoma and osteosarcoma with no involvement of the cartilage. Tissues were obtained from 5 patients (3 males aged 18 (M1), 23 (M2) and 57 (M3) years; 2 females aged 19 (F1) and 68 years (F2)) and chondrocytes were isolated as described previously [26]. The cells were grown and maintained in DMEM/F12 media supplemented with 10% FBS at 37°C with 5% CO_2. Both primary and passaged ($<$3 times) human cells were used in the study.

Cell-survival assay

Human chondrocytes were grown on 24 well plate with DMEM/F12 containing 10% FBS. Once the cells reached 90% confluency, the medium was removed, and the cells were rested in 0.4 ml of serum-free (SF) DMEM/F12 for 1 day. The cells were then incubated with 0.4 ml of fresh SF DMEM/F12 in the absence or presence of 10 nM full-length sLRP1 (BioMac) or 500 nM RAP for 0−72 h. Cell images were acquired by Nikon Eclipse Ti-E and Diaphot with ToupCam camera (Nikon, Tokyo, Japan). Cell viability was measured by MTS cell proliferation colorimetric assay (CellTiter 96® AQueous One Solution Cell Proliferation Assay system, Promega, G3582, Italy). MTS reagents were directly added to the culture of chondrocytes to measure cell viability of both attached and floating detached cells. The number of attached cells were counted by haemocytometer (Hausser Scientific, PA, USA) following washing the cells with serum-free medium and trypsinization. For the experiment using sLRP1-II, cells were maintained on 48 well plate and incubated with 0.2 ml of SF DMEM/F12 in the absence or presence of 0−40 nM sLRP1-II for 24 h.

Sample preparation for secretome analysis

Human chondrocytes were grown on 12 well plate in DMEM/F12 containing 10% FBS. Once the cells reached 90% confluency, the medium was removed and the cells were rested in 1 ml of SF DMEM/F12 for 1 day. The cells were then incubated with 1 ml of SF DMEM in the absence (control) or presence of 5 nM sLRP1-II for 24 h. The conditioned medium was collected into BSA pre-coated 1.5 ml eppendorf tubes and centrifuged at 1,000 x *g* for 10 min to remove cell debris. The supernatant was used for subsequent mass spectrometry analysis.

Liquid Chromatography with tandem mass spectrometry (LC-MS/MS)

Samples were denatured and reduced in 8 M Urea containing 5 mM dithiothreitol for 1 h, alkylated with 15 mM Iodoacetamide for 1 h and diluted 10-fold with 50 mM NH_4HCO_3. Sequencing grade trypsin was added (1:50 w/w) and the sample was digested overnight 37°C and desalted using self-packed reverse phase micro-columns containing C18 column material (EmporeTM). LC-MS/MS was performed using an EASY-nLC 1000 (Thermo Scientific) connected to an Q Exactive Plus mass spectrometer (Thermo Scientific). The peptides were separated on a 15 cm analytical column (75 μm inner diameter). The column was packed in-house with ReproSil-Pur C18-AQ 3 μm resin (Dr. Maisch GmbH, Ammerbuch-Entringen, Germany). The flow rate were 250 nl/min and a 50 min gradient from 5% to 35% phase B (0.1% formic acid, 90% acetonitrile).

LC-MS/MS data analysis

The acquired MS data were processed in Proteome Discoverer 2.4 (Thermo Scientific). The data was searched against the human proteome (UniProt) using the Sequest HT search engine. Search parameters were trypsin as protease; minimum peptide length of 6 residues; Precursor Mass Tolerance of 10 ppm; Fragment Mass Tolerance of 0.02 Da and dynamic modifications with oxidation on Met. The search results were used for precursor ion quantification without normalization. Statistical analysis using the search results and intensities from Proteome discover was made with Perseus (v1.6.5.0) [121]. Initially the results were filtered based on the Protein false discovery rate (FDR) to remove low confidence IDs. For secretome analysis,

the proteins only identified 1 or 2 out of 4 samples in each condition were removed from the data set. The raw intensities were log2 transformed and missing values were replaced based on the normal distribution of the entire dataset. A two-sample t-test was performed to identify significant changes and calculate the fold change. The proteins identified in all 4 biological replicates of sLRP1-II-treated cells, but only in 0-1 replicates of untreated control cells were categorized as ON molecules. Conversely, the proteins identified in all 4 replicates of control cells, but only in 0-1 replicates of sLRP1-II-treated cells were categorized as OFF molecules. Uniprot database was used for subcellular localization. Volcano plot analysis was performed using GraphPad Prism 9. An adjuster p-value corrected for a FDR was calculated in Perseus using the Benjamini-Hochberg method (FDR < 0.01). Several proteins were identified in the sLRP1-II preparation thereby all intensities were normalized to the intensity of sLRP-II preparation in the sample.

Western blot analysis of secreted proteins produced by human chondrocytes

Human chondrocytes were incubated for 24 h with SF DMEM/F12 containing CT1746 (100 μM) and the protease inhibitor cocktail (1/500) in the presence and the absence of 5 nM sLRP1-II. After incubation, media were collected, and the protein was precipitated with trichloroacetic acid and dissolved in 20 μl of 1x SDS-sample buffer (50 mM Tris-HCl pH 6.8, 5% 2-mercaptoethanol (2ME), 2% SDS and 10% glycerol). All samples were analyzed by SDS-PAGE and Western blotting using a specific antibody against each protein. Immunoreactive bands were quantified using NIH ImageJ, and the relative amount of each ligand in the medium in the presence and absence of sLRP1-II was calculated.

Quantitative reverse transcriptase-polymerase chain reaction (qRT-PCR)

Human chondrocytes were incubated for 24 h with SF DMEM/F12 containing CT1746 (100 μM) and the protease inhibitor cocktail (1/500) in the presence and the absence of 200 nM RAP, 10 nM full-length sLRP1 or 10 nM denatured full-length sLRP1 (preincubated at 98°C for 10 min) for 0-24 h. cDNA was generated from these cells using a reverse-transcription kit (Applied Biosystems, CA, USA) and random primers from RNA extracted and prepared using the RNeasymini kit (Qiagen, CA, USA) following the manufacturer's guidelines. cDNA was then used for real time PCR assays using TaqMan technology. The ΔΔ threshold cycle ($\Delta\Delta C_t$) method of relative quantitation was used to calculate relative mRNA levels for each transcript examined. The 60S acidic ribosomal protein P0 (RPLP0) gene was used to normalize the data. Pre-developed primer/probe sets for MMP1, MMP3, MMP13, ADAMTS4, ADAMTS5, TIMP3 and RPLP0 were purchased from Applied Biosystems.

Isolation of LRP1 ligands in human chondrocytes

Human chondrocytes were grown on 12 well plate in DMEM/F12 containing 10% FBS. Once the cells reached 90% confluency, the medium was removed, and the cells were rested in 1 ml of SF DMEM/F12 for 1 day. The cells were then incubated with 1 ml of SF DMEM containing the broad-spectrum hydroxamate metalloproteinases inhibitor CT1746 (100 μM) and the protease inhibitor cocktail (a mixture of aprotinin, bestatin, E-64, leupeptin and pepstatin A) (SIGMA, P1860) in the absence (control) or presence of 5 nM sLRP1-II for 24 h. The conditioned medium was collected into BSA pre-coated 1.5 ml eppendorf tubes and centrifuged briefly by table-top centrifuge to remove cell debris. 900 μl of the supernatant was collected into new BSA pre-coated 1.5 ml tubes and further incubated with 50 μl of anti-c-Myc paramagnetic Dynabeads at 4°C for 1 h. sLRP1-II and the magnetic beads complexes were then isolated using the magnetic stand, washed with the buffer consisting of 50 mM Tris-HCl (pH 7.5), 150 mM NaCl, 5 mM $CaCl_2$ (TNC), and 0.02% Brij-35 (TNCB) for three times, and eluted with 200 μl of 0.1 M glycine buffer (pH 3.0) for 10 min at 4°C. The eluents were neutralised with 10 μl of 1 M Tris-HCl (pH 8.0).

Purification of full-length sLRP1

LRP1 was purified from human placenta by RAP affinity chromatography [122]. Briefly, for column preparation, C-terminally his-tagged RAP [22] was expressed in *Escherichia coli*, harvested by centrifugation, and resuspended in 50 mM HEPES (pH 7.4) and 150 mM NaCl (HBS) supplemented with complete EDTA-free Protease Inhibitor Cocktail (Roche) prior to lysis by sonication on ice. For RAP purification, the lysate was applied to a HisTrap column (Cytiva Life Sciences), and bound proteins were eluted using a stepwise increase of imidazole concentrations from 12.5−250 mM. A total of 3 mg RAP was coupled to a 1 ml HiTrap NHS-activated HP column (Cytivia Life Sciences) according to the manufacturer's protocol. LRP1 was extracted from fresh human placenta as previously described [123], and the placental mixture was applied to the RAP affinity column equilibrated in HBS with 5 mM CaCl2 and 0.05% Tween. Bound proteins were eluted by 100 mM CH_3COONa (pH 5.0) and 0.5 M NaCl and further purified using a Sephacryl S-300 HR (Cytiva Life Sciences) size exclusion column equilibrated in 100 mM CH_3COONa (pH 5.5) and 150 mM NaCl.

Purification of CEMIP

The expression construct for full-length human CEMIP (Uniprot ID: Q8WUJ3) containing a FLAG tag at the C-terminus in pReceiver-M39 was purchased from GeneCopoeia. HEK293 expressing the SV40 large T antigen were cultured in DMEM/F12 with 10% FBS, 1 U/mL Penicillin and 0.1 mg/mL Streptomycin (Pen/Strep)(Sigma) at 37°C, with 5% CO_2. Constructs were transiently transfected using TransIT2020 (Mirus Bio) following the manufacturer's protocol. After the transfection, cells were incubated for 3 days in the presence of 100 μg/ml heparin from porcine intestinal mucosa (Sigma, H3393) to prevent LRP1-mediated endocytic clearance before harvesting. Conditioned medium (2 L) was harvested and centrifuged for 20 min at 1500 x g, followed by filtration (0.45 μm) to remove cell debris. The conditioned medium was passed over a 2-ml anti-FLAG M2 Affinity Gel (Sigma, A2220) at 4° C. The column was first washed extensively with 50 mM Tris-HCl (pH 7.5) containing 1 M NaCl, 5 mM $CaCl_2$, and 0.02% Brij-35. The bound material was eluted with 200 μg/mL FLAG peptide (Sigma, F3290). The purified samples were then passed through a PD-10 column (GE Healthcare, UK) pre-equilibrated in 50 mM HEPES, 150 mM NaCl, 5 mM $CaCl_2$, and 0.02% Brij-35. Fractions containing pure CEMIP were pooled, concentrated and stored at -80°C before activity assays. Protein concentration was measured using Nanodrop and calculated according to Beer−Lambert law, using extinction coefficient 226,115 $M^{-1}cm^{-1}$ using the Expasy ProtParam web tool.

Purification of fibulin1c

The cDNA coding for fibulin1C (Uniprot number P23142-4) with a C-terminal 6x His tag was custom-synthesized by Invitrogen and transiently transfected in HEK293 T cells using polyethylenimine in OPTIMEM (Invitrogen) containing 2 mM $CaCl_2$. After 72 h, fibulin1C was concentrated 15-fold using a Lab scale TFF system (Merck) and purified using a Ni-sepharose column (GE Healthcare) equilibrated with 3 column volumes TBS (20 mM Tris-HCl (pH 7.4), 150 mM NaCl). Following binding, the column was washed with TBS containing 10 mM imidazole and bound proteins were eluted using a linear gradient (10−300 mM) of imidazole. Eluted fractions containing recombinant proteins were subjected to SDS- polyacrylamide gel electrophoresis (PAGE), pooled, concentrated on Amicon Ultra spin columns (50 kDa cut-off) and dialyzed extensively against TBS. Purified fibulin1C was stored at -80°C. Protein concentration was measured using Nanodrop and calculated according to Beer−Lambert law, using extinction coefficient 35,750 M-1cm-1 using the Expasy ProtParam web tool.

Enzyme-linked immunosorbent assay (ELISA) for the binding of recombinant LRP1 ligand candidate proteins to full-length sLRP1

Purified human full-length LRP1 (10 nM in 100 μl of TNC) was coated overnight at 4°C onto microtiter plates (Corning, NY). Wells were blocked with 3% BSA in TNC (1 h; 37°C) and washed in TNC containing 0.05% Brij-35 after this and each subsequent step. Wells were then incubated with various concentrations of recombinant proteins in blocking solution for 3 h at room temperature. Bound proteins were detected using anti-FLAG M2 antibody or anti-His tag antibody (1 h; room temperature) and then with a secondary antibody coupled to horseradish peroxidase (1 h; room temperature). Hydrolysis of tetramethylbenzidine substrate (KPL, Gaithersburg, MA) was measured at 450 nm using a FLUOstar Omega (BMG Labtech). Mean values of technical duplicate were normalized by subtracting the amount of recombinant protein bound to control well that was not coated with LRP1. Extrapolated $K_{D,app}$ values were estimated based on one-phase decay nonlinear fit analysis using GraphPad Prism 9.

Endocytosis assay using WT and LRP1 deficient MEFs

WT and LRP1 KO MEFs were generated as described previously [43] and kindly provided by Professor Dudley Strickland (University of Maryland School of Medicine). Cells (1×10^4/well) cultured in 96-well plates (pre-coated with 0.1% gelatin for 3 h) were rested in 100 μl of DMEM for 1 day. The medium was replaced with 50 μl of fresh DMEM containing recombinant proteins (20 nM). After 8 h, 30 μl of medium were collected and mixed with 10 μl of 4x SDS-sampling buffer (200 mM Tris-HCl (pH 6.8), 8% SDS and 40% glycerol) containing 10% 2ME. The medium was then completely removed, and the cells were lysed with 50 μl of 2x SDS-sampling buffer containing 5% 2ME. All samples were analyzed by SDS-PAGE under reducing conditions and immunoblotting using anti-His tag or anti-FLAG M2 antibody. Immune signals for exogenously added proteins in the medium were quantified using ImageJ and the amount of the protein remaining in the medium after 8 h incubation was calculated as a percentage of the amount before incubation.

Immunocytochemical localization of newly identified LRP1 ligands

Human chondrocytes were grown on 8-well Lab-Tek chamber slides (Nunc Lab-Tek Chamber Slide System, Thermo Scientific) with DMEM/F12 containing 10% FBS. Once reaching confluency, the cells were rested in serum free DMEM/F12 medium for

24 h. Cells were then incubated in DMEM/F12 with 10 nM CEMIP (FLAG tag at C-terminus), 20 nM HMGB2 (His-tag at C-terminus), 20 nM SLIT2 (His-tag at C-terminus) or 20 nM ADAMTS1 (FLAG tag at C-terminus) in the presence or absence of 500 nM RAP or 40 nM sLRP1 for 1 h at 37°C. Cells were washed with DMEM/F12 for three times, fixed with 3% paraformaldehyde in PBS for 10 min, permeabilized with in TNC containing 0.1% Triton X-100 (4 min, room temperature). Each sample was incubated with anti-FLAG M2 mouse monoclonal antibody (for CEMIP and ADAMTS1) or anti-His tag antibody (for HMGB2 and SLIT2) and anti-EEA1 rabbit polyclonal antibody (2 h, room temperature). Cells were washed with TNC for three times and further incubated with Alexa Fluor 488-conjugated anti-mouse IgG and Alexa Fluor 568-conjugated anti-rabbit IgG (Molecular Probes, Eugene, OR) to visualize the antigen signals (1 h, room temperature). Actin was stained with Actin-stain 670 phalloidin (Cell Signalling). Cells were washed with TNC for three times and mounted with ProLong Diamond Antifade Mountant with DAPI (Thermo Fisher). Immunofluorescence images were acquired using a Zeiss LSM 800 confocal microscope (Zeiss, Oberkochen, Germany). Images were processed using either Zen 2.6 (blue edition, Zeiss).

Establishment of pan-tissue LRP1 conditional knockout mice

$LRP^{flox/flox}$ (129S7-$Lrp1^{tm2Her}$/J) mutant mice carrying a floxed Neo cassette and a single loxP site downstream of exon2 of the targeted *LRP1* gene, were crossed with tamoxifen-inducible *Cre* recombinase transgene R26CreERT2 (129-Gt (ROSA) $26Sor^{tm1(cre/ERT2)Tyj}$/J) mice to generate LRP1 conditional pan tissue KO mice. Both were provided by The Jackson Laboratory (012604 and 008463). Fifty mg tamoxifen free base (Sigma, T5648) was suspended in 500 μl 100% ethanol, diluted and fully dissolved in 4,500 μl of corn oil (Sigma, C8267) by sonication (final 10 mg/ml). 5-6 months-old mice were administrated 40 mg tamoxifen/Kg body weight by intraperitoneal injections for three times over a week with 2- and 4-days interval.

Genotyping

Four weeks after birth, ear notches were collected from mouse pups to extract genomic DNA using the RED Extract-N-Amp Tissue PCR Kit (Sigma-Aldrich). Ear notches were incubated in the tissue preparation (25 μl/sample) and extraction solutions (100 μl/sample) at room temperature for 10 min. Ear notches were heated to 95°C for 3 min and later mixed with the neutralization solution (100 μl/sample) to offset inhibitory substances before PCR. Samples were kept at 4°C until PCR. For R26-Cre ERT2 mouse genotyping, 300 ng of genomic DNA was mixed with 0.2 μl of Go Taq®G2 flexi DNA polymerase (PROMEGA), 5.0 μl of 5X Green Go Taq ® Flexi buffer (PROMEGA), 3.0 μl MgCl2 (25mM) (PROMEGA), 1.0 μl dNTPs (100 mM, Meridian), 0.5 μl (20 μM) of each primer and nuclease-free water was added to make the reaction mixture up to 25 μl. Primer pairs for genotyping were as follows; ROSA Cre WT Forward (21306) 5' - CTG GCT TCT GAG GAC CG - 3', ROSA Cre WT Reverse (oIMR9021) 5'- CCG AAA ATC TGT GGG AAGTC - 3', ROSA Cre Mut. Forward (oIMR3621) 5'- CGT GAT CTG CAA CTC CAG TC- 3', ROSA Cre Mut. Reverse (oIMR9074) 5'- AGG CAA ATT TTG GTG TAC GG - 3'. Cycle conditions were as follows: Genotyping - 1 cycle of 94°C for 2 min, 10 cycles of 94°C for 20 s; 65°C for 15 s (-0.5°C per cycle) (touchdown); 68°C for 10 s, and 28 cycles of 94°C for 15 s; 60°C for 15 s; 72°C for 10 s, followed by a final cycle of 72°C for 2 min. PCR products were separated by gel electrophoresis and imaged using a BioRad Gel Doc XR+ System. For LRP1 floxed mice mouse genotyping, 100 ng of genomic DNA was mixed with 10 μl of REDExtract-N-Amp™ PCR ReadyMix™, 0.5 μl (20 μM) of each primer and nuclease-free water was added to make the reaction mixture up to 20 μl. Primer pairs for genotyping were as follows; LRP1 Flox forward 5'- CATA-CCCTCTTCAAACCCCTTCCTG - 3', LRP1 Flox Reverse 5'- GCAAGCTCTCCTGCTCAGACCTGGA - 3'. Cycle conditions were as follows: Genotyping −1 cycle of 94°C for 3 min, 35 cycles of 94°C for 30 s; 65°C for 30 s; 72°C for 30 s, followed by a final cycle of 72°C for 2 min. PCR products were separated by gel electrophoresis and imaged using a Bio-Rad Gel Doc XR+ System.

Tissue processing for histology

Animals were euthanized by CO_2 and knee joints were removed by using sanitized scissors. The tissues were fixed in 4% paraformaldehyde for 24 h, stored in 70% ethanol followed by decalcification with 10% EDTA (pH 8.0) for 2 weeks. The decalcified tissues were then processed through graded ethanol and xylene before being embedded in paraffin wax. 4.5 μm sections were cut using a rotary microtome RM2235 (Leica), adhered to microscope slides, then dried overnight at 37°C. Sections were dewaxed and rehydrated with xylene followed by a series of decreasing ethanol concentrations prior to the histological analysis.

Immunohistochemical staining of LRP1 and LRP1 ligands

Slides were incubated with the basic-based antigen unmasking solution by placing a polypropylene Coplin staining jar filled with the respective retrieval

solution into a water bath at 92−95°C for 3−8 min. Slides were washed with distilled water followed by PBS and blocked with 0.3% hydrogen peroxide for 15 min at 37 °C. Slides were then incubated with Avidin solution for 15 min followed by the Biotin solution for 15 min at room temperature. After washing with PBS, slides were incubated with PBS containing 10% goat serum and 0.1% BSA for 3 h at room temperature. Slides were then incubated with anti-LRP1 β-chain rabbit monoclonal antibody (ab92544), anti-SLIT2 rabbit monoclonal antibody (ab134166), anti-CEMIP rabbit polyclonal antibody (21129-1-AP) or anti-CCN2 rabbit polyclonal antibody (ab6992) overnight at 4 °C. Rabbit IgG was used as an isotype control. Slides were washed with PBS containing 0.1% Tween 20 (PBST) three times for 10 min each. Slides were then incubated with secondary antibody ImmPRESS peroxidase-micropolymer conjugated horse anti-rabbit IgG for 30 min at room temperature followed by incubation with Vectastain solution (Vector Labs, PK-6100) for 30 min at room temperature. After wash with PBST three times for 10 min each slide was stained with 3,3'-diaminobenzidine and counterstained with Methyl green solution for 5 min followed by dehydration and mounted with DPX mounting media. Images were acquired using a Nikon Eclipse Ti-E microscope (Nikon, Tokyo, Japan).

CRediT authorship contribution statement

Kazuhiro Yamamoto: Visualization, Data curation, Writing – review & editing. Carsten Scavenius : Writing –review & editing, Investigation, Data curation. **Maria M Meschis:** Writing – review & editing, Investigation, Data curation. **Abdulrahman M E Gremida:** Writing – review & editing, Investigation, Data curation. **Emilie H Mogensen:** Writing – review & editing, Investigation, Data curation. **Ida B Thøgersen:** Writing – review & editing, Investigation, Data curation. **Simone Bonelli:** Writing – review & editing, Formal analysis. **Simone D Scilabra:** Writing – review & editing, Formal analysis. **Anders Jensen:** Investigation, Writing – review & editing. **Salvatore Santamaria:** Writing – review & editing, Investigation. **Josefin Ahnström:** Writing – review & editing, Investigation. **George Bou-Gharios:** Investigation, Writing – review & editing. **Jan J Enghild:** Investigation, Writing – review & editing. **Hideaki Nagase:** Investigation, Writing – review & editing.

Declaration of Competing Interest

The authors declare that there are no conflicts of interests.

Acknowledgments

We are grateful to the staff at the University of Liverpool Biomedical Services and Histology Units. We thank Dr Jaysh Dudhia (Royal Veterinary College, United Kingdom) for providing human normal cartilage. This work was supported by the Versus Arthritis (21447 to K.Y.) and the University of Liverpool Crossley Barnes Bequest fund (K.Y. and M.M.M.), the British Heart Foundation (FS/IBSRF/20/25032 to S.S.), a "Fondazione con il Sud" grant within the Brains to South program (2018-PDR-0799 to S.B. and S.D.S.), the VELUX FONDEN (00014557 to J.J. E.), the Danish Council for Independent Research-Medical Science (DFF-4004-00471 to J.J.E.), and the LEO Foundation and the Novo Nordisk Foundation (BIO-MS)(NNF18OC0032724 to J.J.E.).

Supplementary materials

Supplementary material associated with this article can be found in the online version at doi:10.1016/j.matbio.2022.08.007.

Received 11 March 2022;
Received in revised form 26 July 2022;
Accepted 17 August 2022
Available online 24 August 2022

Keywords:
Endocytosis;
LRP1;
Extracellular matrix;
Interactome;
Chondrocyte;
Cartilage;
Osteoarthritis

Abbreviations:
LRP1, low-density lipoprotein receptor-related protein 1; SLIT2, slit homolog 2 protein; CEMIP, cell migration-inducing and hyaluronan-binding protein; ECM, extracellular matrix; SMCs, smooth muscle cells; OA, osteoarthritis; TIMP, tissue inhibitor of metalloproteinase; MMP, matrix metalloproteinase; ADAM, a disintegrin and metalloproteinase; ADAMTS, ADAM with thrombospondin motifs; RAP, receptor-associated protein; HMG, high mobility group protein; HGFA, hepatocyte growth factor activator; IGFBP, insulin-like growth factor-binding protein; TNF, tumor necrosis factor; TSG6, TNF-inducible gene 6 protein; SPARC, secreted protein acidic and rich in cysteine; WT, wild-type; KO, knockout; MEFs, mouse embryonic fibroblasts; CTGF, connective tissue growth factor; GAGs, glycosaminoglycans; Lef-1, lymphoid enhancer-binding factor 1; IαI, inter-α-inhibitor; FBS, fetal bovine serum; BSA, bovine serum albumin; DMEM/F12, Dulbecco's Modified Eagle's Medium/Nutrient Mixture F-12 Ham; SF, serum-free; LC-MS/MS, liquid Chromatography with

tandem mass spectrometry; SDS, sodium dodecyl sulphate; PAGE, polyacrylamide gel electrophoresis; 2ME, 2-mercaptoethanol; qRT-PCR, quantitative reverse transcriptase-polymerase chain reaction

References

[1] S.K. Moestrup, J. Gliemann, G. Pallesen, Distribution of the alpha 2-macroglobulin receptor/low density lipoprotein receptor-related protein in human tissues, Cell Tissue Res. 269 (3) (1992) 375–382.

[2] G. Zheng, D.R. Bachinsky, I. Stamenkovic, D.K. Strickland, D. Brown, G. Andres, R.T. McCluskey, Organ distribution in rats of two members of the low-density lipoprotein receptor gene family, gp330 and LRP/alpha 2MR, and the receptor-associated protein (RAP), J. Histochem. Cytochem. 42 (4) (1994) 531–542.

[3] D.K. Strickland, S.L. Gonias, W.S. Argraves, Diverse roles for the LDL receptor family, Trends Endocrinol. Metab. 13 (2) (2002) 66–74.

[4] E.E. Bres, A. Faissner, Low density receptor-related protein 1 interactions with the extracellular matrix: more than meets the eye, Front. Cell Dev. Biol. 7 (2019) 31.

[5] D.T. Au, A.L. Arai, W.E. Fondrie, S.C. Muratoglu, D.K. Strickland, Role of the LDL receptor-related protein 1 in regulating protease activity and signaling pathways in the vasculature, Curr. Drug Targets 19 (11) (2018) 1276–1288.

[6] J. Herz, D.E. Clouthier, R.E. Hammer, LDL receptor-related protein internalizes and degrades uPA-PAI-1 complexes and is essential for embryo implantation, Cell 71 (3) (1992) 411–421.

[7] C. Nakajima, P. Haffner, S.M. Goerke, K. Zurhove, G. Adelmann, M. Frotscher, J. Herz, H.H. Bock, P. May, The lipoprotein receptor LRP1 modulates sphingosine-1-phosphate signaling and is essential for vascular development, Development 141 (23) (2014) 4513–4525.

[8] P. May, A. Rohlmann, H.H. Bock, K. Zurhove, J.D. Marth, E.D. Schomburg, J.L. Noebels, U. Beffert, J.D. Sweatt, E.J. Weeber, J. Herz, Neuronal LRP1 functionally associates with postsynaptic proteins and is required for normal motor function in mice, Mol. Cell. Biol. 24 (20) (2004) 8872–8883.

[9] L. Hu, L.S. Boesten, P. May, J. Herz, N. Bovenschen, M.V. Huisman, J.F. Berbee, L.M. Havekes, B.J. van Vlijmen, J.T. Tamsma, Macrophage low-density lipoprotein receptor-related protein deficiency enhances atherosclerosis in ApoE/LDLR double knockout mice, Arterioscler. Thromb. Vasc. Biol. 26 (12) (2006) 2710–2715.

[10] C.D. Overton, P.G. Yancey, A.S. Major, M.F. Linton, S. Fazio, Deletion of macrophage LDL receptor-related protein increases atherogenesis in the mouse, Circ. Res. 100 (5) (2007) 670–677.

[11] A.N. Hamlin, J.E. Basford, A. Jaeschke, D.Y. Hui, LRP1 protein deficiency exacerbates palmitate-induced steatosis and toxicity in hepatocytes, J. Biol. Chem. 291 (32) (2016) 16610–16619.

[12] Y. Ding, X. Xian, W.L. Holland, S. Tsai, J. Herz, Low-density lipoprotein receptor-related protein-1 protects against hepatic insulin resistance and hepatic steatosis, EBioMedicine 7 (2016) 135–145.

[13] P. Boucher, M. Gotthardt, W.P. Li, R.G. Anderson, J. Herz, LRP: role in vascular wall integrity and protection from atherosclerosis, Science 300 (5617) (2003) 329–332.

[14] S.C. Muratoglu, S. Belgrave, B. Hampton, M. Migliorini, T. Coksaygan, L. Chen, I. Mikhailenko, D.K. Strickland, LRP1 protects the vasculature by regulating levels of connective tissue growth factor and HtrA1, Arterioscler. Thromb. Vasc. Biol. 33 (9) (2013) 2137–2146.

[15] H. Mao, P. Lockyer, W.H. Townley-Tilson, L. Xie, X. Pi, LRP1 regulates retinal angiogenesis by inhibiting PARP-1 activity and endothelial cell proliferation, Arterioscler. Thromb. Vasc. Biol. 36 (2) (2016) 350–360.

[16] S.M. Hofmann, L. Zhou, D. Perez-Tilve, T. Greer, E. Grant, L. Wancata, A. Thomas, P.T. Pfluger, J.E. Basford, D. Gilham, J. Herz, M.H. Tschop, D.Y. Hui, Adipocyte LDL receptor-related protein-1 expression modulates postprandial lipid transport and glucose homeostasis in mice, J. Clin. Investig. 117 (11) (2007) 3271–3282.

[17] D.T. Au, D.K. Strickland, S.C. Muratoglu, The LDL receptor-related protein 1: at the crossroads of lipoprotein metabolism and insulin signaling, J. Diabetes Res. 2017 (2017) 8356537.

[18] B. Van Gool, S. Dedieu, H. Emonard, A.J. Roebroek, The matricellular receptor LRP1 forms an interface for signaling and endocytosis in modulation of the extracellular tumor environment, Front. Pharmacol. 6 (2015) 271.

[19] K. Yamamoto, S. Santamaria, K.A. Botkjaer, J. Dudhia, L. Troeberg, Y. Itoh, G. Murphy, H. Nagase, Inhibition of shedding of low-density lipoprotein receptor-related protein 1 reverses cartilage matrix degradation in osteoarthritis, Arthritis Rheumatol. 69 (6) (2017) 1246–1256.

[20] M.B. Goldring, F. Berenbaum, Emerging targets in osteoarthritis therapy, Curr. Opin. Pharmacol. 22 (2015) 51–63.

[21] K. Yamamoto, K. Owen, A.E. Parker, S.D. Scilabra, J. Dudhia, D.K. Strickland, L. Troeberg, H. Nagase, Low density lipoprotein receptor-related protein 1 (LRP1)-mediated endocytic clearance of a disintegrin and metalloproteinase with thrombospondin motifs-4 (ADAMTS-4): functional differences of non-catalytic domains of ADAMTS-4 and ADAMTS-5 in LRP1 binding, J. Biol. Chem. 289 (10) (2014) 6462–6474.

[22] K. Yamamoto, L. Troeberg, S.D. Scilabra, M. Pelosi, C.L. Murphy, D.K. Strickland, H. Nagase, LRP-1-mediated endocytosis regulates extracellular activity of ADAMTS-5 in articular cartilage, FASEB J. 27 (2) (2013) 511–521.

[23] K. Yamamoto, H. Okano, W. Miyagawa, R. Visse, Y. Shitomi, S. Santamaria, J. Dudhia, L. Troeberg, D.K. Strickland, S. Hirohata, H. Nagase, MMP-13 is constitutively produced in human chondrocytes and co-endocytosed with ADAMTS-5 and TIMP-3 by the endocytic receptor LRP1, Matrix Biol. 56 (2016) 57–73.

[24] A.P. Carreca, V.M. Pravata, M. Markham, S. Bonelli, G. Murphy, H. Nagase, L. Troeberg, S.D. Scilabra, TIMP-3 facilitates binding of target metalloproteinases to the endocytic receptor LRP-1 and promotes scavenging of MMP-1, Sci. Rep. 10 (1) (2020) 12067.

[25] S.D. Scilabra, L. Troeberg, K. Yamamoto, H. Emonard, I. Thogersen, J.J. Enghild, D.K. Strickland, H. Nagase, Differential regulation of extracellular tissue inhibitor of metalloproteinases-3 levels by cell membrane-bound and shed low density lipoprotein receptor-related protein 1, J. Biol. Chem. 288 (1) (2013) 332–342.

[26] L. Troeberg, K. Fushimi, R. Khokha, H. Emonard, P. Ghosh, H. Nagase, Calcium pentosan polysulfate is a

multifaceted exosite inhibitor of aggrecanases, FASEB J. 22 (10) (2008) 3515–3524.
[27] M. Gorovoy, A. Gaultier, W.M. Campana, G.S. Firestein, S.L. Gonias, Inflammatory mediators promote production of shed LRP1/CD91, which regulates cell signaling and cytokine expression by macrophages, J. Leukoc. Biol. 88 (4) (2010) 769–778.
[28] D.V. Rozanov, E. Hahn-Dantona, D.K. Strickland, A.Y. Strongin, The low density lipoprotein receptor-related protein LRP is regulated by membrane type-1 matrix metalloproteinase (MT1-MMP) proteolysis in malignant cells, J. Biol. Chem. 279 (6) (2004) 4260–4268.
[29] C. Selvais, L. D'Auria, D. Tyteca, G. Perrot, P. Lemoine, L. Troeberg, S. Dedieu, A. Noel, H. Nagase, P. Henriet, P.J. Courtoy, E. Marbaix, H. Emonard, Cell cholesterol modulates metalloproteinase-dependent shedding of low-density lipoprotein receptor-related protein-1 (LRP-1) and clearance function, FASEB J. 25 (8) (2011) 2770–2781.
[30] A. Fernandez-Castaneda, S. Arandjelovic, T.L. Stiles, R.K. Schlobach, K.A. Mowen, S.L. Gonias, A. Gaultier, Identification of the low density lipoprotein (LDL) receptor-related protein-1 interactome in central nervous system myelin suggests a role in the clearance of necrotic cell debris, J. Biol. Chem. 288 (7) (2013) 4538–4548.
[31] S. Santamaria, K. Yamamoto, K. Botkjaer, C. Tape, M.R. Dyson, J. McCafferty, G. Murphy, H. Nagase, Antibody-based exosite inhibitors of ADAMTS-5 (aggrecanase-2), Biochem. J. 471 (3) (2015) 391–401.
[32] J.E. Croy, W.D. Shin, M.F. Knauer, D.J. Knauer, E.A. Komives, All three LDL receptor homology regions of the LDL receptor-related protein bind multiple ligands, Biochemistry 42 (44) (2003) 13049–13057.
[33] A.B. Meijer, J. Rohlena, C. van der Zwaan, A.J. van Zonneveld, R.C. Boertjes, P.J. Lenting, K. Mertens, Functional duplication of ligand-binding domains within low-density lipoprotein receptor-related protein for interaction with receptor associated protein, alpha2-macroglobulin, factor IXa and factor VIII, Biochim. Biophys. Acta 1774 (6) (2007) 714–722.
[34] J.G. Neels, B.M. van Den Berg, A. Lookene, G. Olivecrona, H. Pannekoek, A.J. van Zonneveld, The second and fourth cluster of class A cysteine-rich repeats of the low density lipoprotein receptor-related protein share ligand-binding properties, J. Biol. Chem. 274 (44) (1999) 31305–31311.
[35] S.D. Scilabra, K. Yamamoto, M. Pigoni, K. Sakamoto, S.A. Muller, A. Papadopoulou, S.F. Lichtenthaler, L. Troeberg, H. Nagase, K. Kadomatsu, Dissecting the interaction between tissue inhibitor of metalloproteinases-3 (TIMP-3) and low density lipoprotein receptor-related protein-1 (LRP-1): Development of a "TRAP" to increase levels of TIMP-3 in the tissue, Matrix Biol. 59 (2017) 69–79.
[36] E. Mantuano, C. Brifault, M.S. Lam, P. Azmoon, A.S. Gilder, S.L. Gonias, LDL receptor-related protein-1 regulates NFkappaB and microRNA-155 in macrophages to control the inflammatory response, Proc. Natl. Acad. Sci. USA 113 (5) (2016) 1369–1374.
[37] L. Troeberg, H. Nagase, Proteases involved in cartilage matrix degradation in osteoarthritis, Biochim. Biophys. Acta 1824 (1) (2012) 133–145.
[38] I. Tchetverikov, L.S. Lohmander, N. Verzijl, T.W. Huizinga, J.M. TeKoppele, R. Hanemaaijer, J. DeGroot, MMP protein and activity levels in synovial fluid from patients with joint injury, inflammatory arthritis, and osteoarthritis, Ann. Rheum. Dis. 64 (5) (2005) 694–698.
[39] H. Mi, D. Ebert, A. Muruganujan, C. Mills, L.P. Albou, T. Mushayamaha, P.D. Thomas, PANTHER version 16: a revised family classification, tree-based classification tool, enhancer regions and extensive API, Nucl. Acids Res. 49 (D1) (2021) D394–D403.
[40] D. Szklarczyk, A.L. Gable, D. Lyon, A. Junge, S. Wyder, J. Huerta-Cepas, M. Simonovic, N.T. Doncheva, J.H. Morris, P. Bork, L.J. Jensen, C.V. Mering, STRING v11: protein-protein association networks with increased coverage, supporting functional discovery in genome-wide experimental datasets, Nucl. Acids Res. 47 (D1) (2019) D607–D613.
[41] S.D. Scilabra, M. Pigoni, V. Pravata, T. Schatzl, S.A. Muller, L. Troeberg, S.F. Lichtenthaler, Increased TIMP-3 expression alters the cellular secretome through dual inhibition of the metalloprotease ADAM10 and ligand-binding of the LRP-1 receptor, Sci. Rep. 8 (1) (2018) 14697.
[42] M. Beaujouin, C. Prebois, D. Derocq, V. Laurent-Matha, O. Masson, S. Pattingre, P. Coopman, N. Bettache, J. Grossfield, R.E. Hollingsworth, H. Zhang, Z. Yao, B.T. Hyman, P. van der Geer, G.K. Smith, E. Liaudet-Coopman, Pro-cathepsin D interacts with the extracellular domain of the beta chain of LRP1 and promotes LRP1-dependent fibroblast outgrowth, J. Cell Sci. 123 (Pt 19) (2010) 3336–3346.
[43] T.E. Willnow, J. Herz, Genetic deficiency in low density lipoprotein receptor-related protein confers cellular resistance to Pseudomonas exotoxin A. Evidence that this protein is required for uptake and degradation of multiple ligands, J. Cell Sci. 107 (Pt 3) (1994) 719–726.
[44] L. Troeberg, C. Lazenbatt, E.K.M.F. Anower, C. Freeman, O. Federov, H. Habuchi, O. Habuchi, K. Kimata, H. Nagase, Sulfated glycosaminoglycans control the extracellular trafficking and the activity of the metalloprotease inhibitor TIMP-3, Chem. Biol. 21 (10) (2014) 1300–1309.
[45] K. Yamamoto, G. Murphy, L. Troeberg, Extracellular regulation of metalloproteinases, Matrix Biol. 44-46 (2015) 255–263.
[46] K. Kawata, T. Eguchi, S. Kubota, H. Kawaki, M. Oka, S. Minagi, M. Takigawa, Possible role of LRP1, a CCN2 receptor, in chondrocytes, Biochem. Biophys. Res. Commun. 345 (2) (2006) 552–559.
[47] K. Kawata, S. Kubota, T. Eguchi, E. Aoyama, N.H. Moritani, S. Kondo, T. Nishida, M. Takigawa, Role of LRP1 in transport of CCN2 protein in chondrocytes, J. Cell Sci. 125 (Pt 12) (2012) 2965–2972.
[48] V.K. Rabiej, T. Pflanzner, T. Wagner, K. Goetze, S.E. Storck, J.A. Eble, S. Weggen, W. Mueller-Klieser, C.U. Pietrzik, Low density lipoprotein receptor-related protein 1 mediated endocytosis of beta1-integrin influences cell adhesion and cell migration, Exp. Cell. Res. 340 (1) (2016) 102–115.
[49] S. Dedieu, B. Langlois, J. Devy, B. Sid, P. Henriet, H. Sartelet, G. Bellon, H. Emonard, L. Martiny, LRP-1 silencing prevents malignant cell invasion despite increased pericellular proteolytic activities, Mol. Cell. Biol. 28 (9) (2008) 2980–2995.
[50] A.W. Orr, C.E. Pedraza, M.A. Pallero, C.A. Elzie, S. Goicoechea, D.K. Strickland, J.E. Murphy-Ullrich, Low density lipoprotein receptor-related protein is a calreticulin coreceptor that signals focal adhesion disassembly, J. Cell Biol. 161 (6) (2003) 1179–1189.
[51] L. Wujak, R.T. Bottcher, O. Pak, H. Frey, E. El Agha, Y. Chen, S. Schmitt, S. Bellusci, L. Schaefer,

N. Weissmann, R. Fassler, M. Wygrecka, Low density lipoprotein receptor-related protein 1 couples beta1 integrin activation to degradation, Cell. Mol. Life Sci. 75 (9) (2018) 1671–1685.
[52] W.M. Campana, X. Li, N. Dragojlovic, J. Janes, A. Gaultier, S.L. Gonias, The low-density lipoprotein receptor-related protein is a pro-survival receptor in Schwann cells: possible implications in peripheral nerve injury, J. Neurosci. 26 (43) (2006) 11197–11207.
[53] E. Yang, H. Zheng, H. Peng, Y. Ding, Lentivirus-induced knockdown of LRP1 induces osteoarthritic-like effects and increases susceptibility to apoptosis in chondrocytes via the nuclear factor-kappaB pathway, Exp. Ther. Med. 10 (1) (2015) 97–105.
[54] P.L. Leslie, D.A. Franklin, Y. Liu, Y. Zhang, p53 regulates the expression of LRP1 and apoptosis through a stress intensity-dependent MicroRNA feedback loop, Cell Rep. 24 (6) (2018) 1484–1495.
[55] A.H. Baker, A.B. Zaltsman, S.J. George, A.C. Newby, Divergent effects of tissue inhibitor of metalloproteinase-1, -2, or -3 overexpression on rat vascular smooth muscle cell invasion, proliferation, and death *in vitro*. TIMP-3 promotes apoptosis, J. Clin. Investig. 101 (6) (1998) 1478–1487.
[56] M. Ahonen, A.H. Baker, V.M. Kahari, Adenovirus-mediated gene delivery of tissue inhibitor of metalloproteinases-3 inhibits invasion and induces apoptosis in melanoma cells, Cancer Res. 58 (11) (1998) 2310–2315.
[57] A.H. Baker, S.J. George, A.B. Zaltsman, G. Murphy, A.C. Newby, Inhibition of invasion and induction of apoptotic cell death of cancer cell lines by overexpression of TIMP-3, Br. J. Cancer 79 (9-10) (1999) 1347–1355.
[58] M. Ahonen, R. Ala-Aho, A.H. Baker, S.J. George, R. Grenman, U. Saarialho-Kere, V.M. Kahari, Antitumor activity and bystander effect of adenovirally delivered tissue inhibitor of metalloproteinases-3, Mol. Ther. 5 (6) (2002) 705–715.
[59] M. Bond, G. Murphy, M.R. Bennett, A. Amour, V. Knauper, A.C. Newby, A.H. Baker, Localization of the death domain of tissue inhibitor of metalloproteinase-3 to the N terminus. Metalloproteinase inhibition is associated with proapoptotic activity, J. Biol. Chem. 275 (52) (2000) 41358–41363.
[60] M. Bond, G. Murphy, M.R. Bennett, A.C. Newby, A.H. Baker, Tissue inhibitor of metalloproteinase-3 induces a Fas-associated death domain-dependent type II apoptotic pathway, J. Biol. Chem. 277 (16) (2002) 13787–13795.
[61] D.C. Kirman, B. Renganathan, W.K. Chui, M.W. Chen, N.A. Kaya, R. Ge, Cell surface nucleolin is a novel ADAMTS5 receptor mediating endothelial cell apoptosis, Cell Death. Dis. 13 (2) (2022) 172.
[62] K. Hishikawa, T. Nakaki, T. Fujii, Connective tissue growth factor induces apoptosis via caspase 3 in cultured human aortic smooth muscle cells, Eur. J. Pharmacol. 392 (1-2) (2000) 19–22.
[63] K. Hishikawa, B.S. Oemar, F.C. Tanner, T. Nakaki, T. Fujii, T.F. Luscher, Overexpression of connective tissue growth factor gene induces apoptosis in human aortic smooth muscle cells, Circulation 100 (20) (1999) 2108–2112.
[64] E. Michishita, G. Garces, J.C. Barrett, I. Horikawa, Upregulation of the KIAA1199 gene is associated with cellular mortality, Cancer Lett. 239 (1) (2006) 71–77.
[65] H.K. Kim, H. Zhang, H. Li, T.T. Wu, S. Swisher, D. He, L. Wu, J. Xu, C.A. Elmets, M. Athar, X.C. Xu, H. Xu, Slit2 inhibits growth and metastasis of fibrosarcoma and squamous cell carcinoma, Neoplasia 10 (12) (2008) 1411–1420.
[66] A. Dallol, D. Morton, E.R. Maher, F. Latif, SLIT2 axon guidance molecule is frequently inactivated in colorectal cancer and suppresses growth of colorectal carcinoma cells, Cancer Res. 63 (5) (2003) 1054–1058.
[67] J. Nousbeck, O. Sarig, N. Avidan, M. Indelman, R. Bergman, M. Ramon, C.D. Enk, E. Sprecher, Insulin-like growth factor-binding protein 7 regulates keratinocyte proliferation, differentiation and apoptosis, J. Investing. Dermatol. 130 (2) (2010) 378–387.
[68] R.Y. Chen, H.X. Chen, P. Jian, L. Xu, J. Li, Y.M. Fan, Y.T. Tu, Intratumoral injection of pEGFC1-IGFBP7 inhibits malignant melanoma growth in C57BL/6J mice by inducing apoptosis and down-regulating VEGF expression, Oncol. Rep. 23 (4) (2010) 981–988.
[69] T. Benatar, W. Yang, Y. Amemiya, V. Evdokimova, H. Kahn, C. Holloway, A. Seth, IGFBP7 reduces breast tumor growth by induction of senescence and apoptosis pathways, Breast Cancer Res. Treat. 133 (2) (2012) 563–573.
[70] N. Taniguchi, B. Carames, L. Ronfani, U. Ulmer, S. Komiya, M.E. Bianchi, M. Lotz, Aging-related loss of the chromatin protein HMGB2 in articular cartilage is linked to reduced cellularity and osteoarthritis, Proc. Natl. Acad. Sci. USA 106 (4) (2009) 1181–1186.
[71] F. Meissner, R.A. Scheltema, H.J. Mollenkopf, M. Mann, Direct proteomic quantification of the secretome of activated immune cells, Science 340 (6131) (2013) 475–478.
[72] X. Zhou, L. Sun, F. Bastos de Oliveira, X. Qi, W.J. Brown, M.B. Smolka, Y. Sun, F. Hu, Prosaposin facilitates sortilin-independent lysosomal trafficking of progranulin, J. Cell Biol. 210 (6) (2015) 991–1002.
[73] A.M. Nicholson, N.A. Finch, M. Almeida, R.B. Perkerson, M. van Blitterswijk, A. Wojtas, B. Cenik, S. Rotondo, V. Inskeep, L. Almasy, T. Dyer, J. Peralta, G. Jun, A.R. Wood, T.M. Frayling, C. Fuchsberger, S. Fowler, T.M. Teslovich, A.K. Manning, S. Kumar, J. Curran, D. Lehman, G. Abecasis, R. Duggirala, C. Pottier, H.A. Zahir, J.E. Crook, A. Karydas, L. Mitic, Y. Sun, D.W. Dickson, G. Bu, J. Herz, G. Yu, B.L. Miller, S. Ferguson, R.C. Petersen, N. Graff-Radford, J. Blangero, R. Rademakers, Prosaposin is a regulator of progranulin levels and oligomerization, Nat. Commun. 7 (2016) 11992.
[74] N.V. Lee, J.C. Rodriguez-Manzaneque, S.N. Thai, W.O. Twal, A. Luque, K.M. Lyons, W.S. Argraves, M.L. Iruela-Arispe, Fibulin-1 acts as a cofactor for the matrix metalloprotease ADAMTS-1, J. Biol. Chem. 280 (41) (2005) 34796–34804.
[75] B. Perbal, C. Martinerie, R. Sainson, M. Werner, B. He, B. Roizman, The C-terminal domain of the regulatory protein NOVH is sufficient to promote interaction with fibulin 1C: a clue for a role of NOVH in cell-adhesion signaling, Proc. Natl. Acad. Sci. USA 96 (3) (1999) 869–874.
[76] S. Santamaria, K. Yamamoto, A. Teraz-Orosz, C. Koch, S.S. Apte, R. de Groot, D.A. Lane, J. Ahnstrom, Exosites in hypervariable loops of ADAMTS spacer domains control substrate recognition and proteolysis, Sci. Rep. 9 (1) (2019) 10914.
[77] S. Santamaria, D.R. Martin, X. Dong, K. Yamamoto, S.S. Apte, J. Ahnstrom, Post-translational regulation and proteolytic activity of the metalloproteinase ADAMTS8, J. Biol. Chem. 297 (5) (2021) 101323.
[78] F. Canals, N. Colome, C. Ferrer, C. Plaza-Calonge Mdel, J.C. Rodriguez-Manzaneque, Identification of substrates of the extracellular protease ADAMTS1 by DIGE proteomic analysis, Proteomics 6 (1) (2006) S28–S35 Suppl.

[79] K. Yamamoto, D. Wilkinson, G. Bou-Gharios, Targeting dysregulation of metalloproteinase activity in osteoarthritis, Calcif. Tissue Int. 109 (2) (2020) 277–290.
[80] N. Taniguchi, Y. Kawakami, I. Maruyama, M. Lotz, HMGB proteins and arthritis, Hum. Cell 31 (1) (2018) 1–9.
[81] P.A. Band, J. Heeter, H.G. Wisniewski, V. Liublinska, C.W. Pattanayak, R.J. Karia, T. Stabler, E.A. Balazs, V.B. Kraus, Hyaluronan molecular weight distribution is associated with the risk of knee osteoarthritis progression, Osteoarthr. Cartil. 23 (1) (2015) 70–76.
[82] R. Sztrolovics, A.D. Recklies, P.J. Roughley, J.S. Mort, Hyaluronate degradation as an alternative mechanism for proteoglycan release from cartilage during interleukin-1beta-stimulated catabolism, Biochem. J. 362 (Pt 2) (2002) 473–479.
[83] H. Yoshida, A. Nagaoka, A. Kusaka-Kikushima, M. Tobiishi, K. Kawabata, T. Sayo, S. Sakai, Y. Sugiyama, H. Enomoto, Y. Okada, S. Inoue, KIAA1199, a deafness gene of unknown function, is a new hyaluronan binding protein involved in hyaluronan depolymerization, Proc. Natl. Acad. Sci. USA 110 (14) (2013) 5612–5617.
[84] T. Ohtsuki, O.F. Hatipoglu, K. Asano, J. Inagaki, K. Nishida, S. Hirohata, Induction of CEMIP in chondrocytes by inflammatory cytokines: underlying mechanisms and potential involvement in osteoarthritis, Int. J. Mol. Sci. 21 (9) (2020).
[85] Q.H. Ding, Y.Y. Qi, X.M. Li, W.P. Chen, X.H. Wang, X.W. Ji, Knockdown of KIAA1199 suppresses IL-1beta-induced cartilage degradation and inflammatory responses in human chondrocytes through the Wnt/beta-catenin signalling pathway, Int. Immunopharmacol. 73 (2019) 203–211.
[86] C. Deroyer, E. Charlier, S. Neuville, O. Malaise, P. Gillet, W. Kurth, A. Chariot, M. Malaise, D. de Seny, CEMIP (KIAA1199) induces a fibrosis-like process in osteoarthritic chondrocytes, Cell Death Dis. 10 (2) (2019) 103.
[87] M. Momoeda, S. de Vega, H. Kaneko, C. Yoshinaga, M. Shimoda, T. Nakamura, Y. Endo, H. Yoshida, K. Kaneko, M. Ishijima, Y. Okada, Deletion of hyaluronan-binding protein involved in hyaluronan depolymerization (HYBID) results in attenuation of osteoarthritis in mice, Am. J. Pathol. 191 (11) (2021) 1986–1998.
[88] H. Shimizu, M. Shimoda, S. Mochizuki, Y. Miyamae, H. Abe, M. Chijiiwa, H. Yoshida, J. Shiozawa, M. Ishijima, K. Kaneko, A. Kanaji, M. Nakamura, Y. Toyama, Y. Okada, Hyaluronan-binding protein involved in hyaluronan depolymerization is Up-regulated and involved in hyaluronan degradation in human osteoarthritic cartilage, Am. J. Pathol. 188 (9) (2018) 2109–2119.
[89] J. Shiozawa, S. de Vega, M.Z. Cilek, C. Yoshinaga, T. Nakamura, S. Kasamatsu, H. Yoshida, H. Kaneko, M. Ishijima, K. Kaneko, Y. Okada, Implication of HYBID (Hyaluronan-Binding Protein Involved in Hyaluronan Depolymerization) in hyaluronan degradation by synovial fibroblasts in patients with knee osteoarthritis, Am. J. Pathol. 190 (5) (2020) 1046–1058.
[90] S. Omoto, K. Nishida, Y. Yamaai, M. Shibahara, T. Nishida, T. Doi, H. Asahara, T. Nakanishi, H. Inoue, M. Takigawa, Expression and localization of connective tissue growth factor (CTGF/Hcs24/CCN2) in osteoarthritic cartilage, Osteoarthr. Cartil. 12 (10) (2004) 771–778.
[91] H. Yoshida, A. Nagaoka, S. Nakamura, Y. Sugiyama, Y. Okada, S. Inoue, Murine homologue of the human KIAA1199 is implicated in hyaluronan binding and depolymerization, FEBS Open Bio 3 (2013) 352–356.
[92] T.H. Lee, H.G. Wisniewski, J. Vilcek, A novel secretory tumor necrosis factor-inducible protein (TSG-6) is a member of the family of hyaluronate binding proteins, closely related to the adhesion receptor CD44, J. Cell Biol. 116 (2) (1992) 545–557.
[93] C.H. Chou, M.T. Lee, I.W. Song, L.S. Lu, H.C. Shen, C.H. Lee, J.Y. Wu, Y.T. Chen, V.B. Kraus, C.C. Wu, Insights into osteoarthritis progression revealed by analyses of both knee tibiofemoral compartments, Osteoarthr. Cartil. 23 (4) (2015) 571–580.
[94] M.T. Bayliss, S.L. Howat, J. Dudhia, J.M. Murphy, F.P. Barry, J.C. Edwards, A.J. Day, Up-regulation and differential expression of the hyaluronan-binding protein TSG-6 in cartilage and synovium in rheumatoid arthritis and osteoarthritis, Osteoarthr. Cartil. 9 (1) (2001) 42–48.
[95] C. Fulop, S. Szanto, D. Mukhopadhyay, T. Bardos, R.V. Kamath, M.S. Rugg, A.J. Day, A. Salustri, V.C. Hascall, T.T. Glant, K. Mikecz, Impaired cumulus mucification and female sterility in tumor necrosis factor-induced protein-6 deficient mice, Development 130 (10) (2003) 2253–2261.
[96] H. He, S. Zhang, S. Tighe, J. Son, S.C.G. Tseng, Immobilized heavy chain-hyaluronic acid polarizes lipopolysaccharide-activated macrophages toward M2 phenotype, J. Biol. Chem. 288 (36) (2013) 25792–25803.
[97] C.A. de la Motte, V.C. Hascall, J. Drazba, S.K. Bandyopadhyay, S.A. Strong, Mononuclear leukocytes bind to specific hyaluronan structures on colon mucosal smooth muscle cells treated with polyinosinic acid: polycytidylic acid: inter-alpha-trypsin inhibitor is crucial to structure and function, Am. J. Pathol. 163 (1) (2003) 121–133.
[98] C.H. Chou, D.E. Attarian, H.G. Wisniewski, P.A. Band, V.B. Kraus, TSG-6 - a double-edged sword for osteoarthritis (OA), Osteoarthr. Cartil. 26 (2) (2018) 245–254.
[99] C. Scavenius, E.C. Poulsen, I.B. Thogersen, M. Roebuck, S. Frostick, G. Bou-Gharios, K. Yamamoto, B. Deleuran, J.J. Enghild, Matrix-degrading protease ADAMTS-5 cleaves inter-alpha-inhibitor and releases active heavy chain 2 in synovial fluids from arthritic patients, J. Biol. Chem. 294 (42) (2019) 15495–15504.
[100] D.T. Au, M. Migliorini, D.K. Strickland, S.C. Muratoglu, Macrophage LRP1 promotes diet-induced hepatic inflammation and metabolic dysfunction by modulating Wnt signaling, Mediat. Inflamm. 2018 (2018) 7902841.
[101] J. Terrand, V. Bruban, L. Zhou, W. Gong, Z. El Asmar, P. May, K. Zurhove, P. Haffner, C. Philippe, E. Woldt, R.L. Matz, C. Gracia, D. Metzger, J. Auwerx, J. Herz, P. Boucher, LRP1 controls intracellular cholesterol storage and fatty acid synthesis through modulation of Wnt signaling, J. Biol. Chem. 284 (1) (2009) 381–388.
[102] E.P. Dennis, S.M. Edwards, R.M. Jackson, C.L. Hartley, D. Tsompani, M. Capulli, A. Teti, R.P. Boot-Handford, D.A. Young, K.A. Pirog, M.D. Briggs, CRELD2 Is a novel LRP1 chaperone that regulates noncanonical WNT signaling in skeletal development, J. Bone Miner. Res. 35 (8) (2020) 1452–1469.
[103] A. Zilberberg, A. Yaniv, A. Gazit, The low density lipoprotein receptor-1, LRP1, interacts with the human frizzled-1 (HFz1) and down-regulates the canonical Wnt signaling pathway, J. Biol. Chem. 279 (17) (2004) 17535–17542.
[104] N. Taniguchi, B. Carames, Y. Kawakami, B.A. Amendt, S. Komiya, M. Lotz, Chromatin protein HMGB2 regulates articular cartilage surface maintenance via beta-catenin pathway, Proc. Natl. Acad. Sci. USA 106 (39) (2009) 16817–16822.

[105] L. Chen, K. Shi, T.L. Andersen, W. Qiu, M. Kassem, KIAA1199 is a secreted molecule that enhances osteoblastic stem cell migration and recruitment, Cell Death Dis. 10 (2) (2019) 126.
[106] H. Blockus, A. Chedotal, Slit-Robo signaling, Development 143 (17) (2016) 3037–3044.
[107] J.M. Rothberg, J.R. Jacobs, C.S. Goodman, S. Artavanis-Tsakonas, Slit: an extracellular protein necessary for development of midline glia and commissural axon pathways contains both EGF and LRR domains, Genes Dev. 4 (12A) (1990) 2169–2187.
[108] J.M. Rothberg, D.A. Hartley, Z. Walther, S. Artavanis-Tsakonas, slit: an EGF-homologous locus of D. Melanogaster involved in the development of the embryonic central nervous system, Cell 55 (6) (1988) 1047–1059.
[109] K. Miyazawa, T. Shimomura, A. Kitamura, J. Kondo, Y. Morimoto, N. Kitamura, Molecular cloning and sequence analysis of the cDNA for a human serine protease reponsible for activation of hepatocyte growth factor. Structural similarity of the protease precursor to blood coagulation factor XII, J. Biol. Chem. 268 (14) (1993) 10024–10028.
[110] H. Itoh, S. Naganuma, N. Takeda, S. Miyata, S. Uchinokura, T. Fukushima, S. Uchiyama, H. Tanaka, K. Nagaike, T. Shimomura, K. Miyazawa, G. Yamada, N. Kitamura, M. Koono, H. Kataoka, Regeneration of injured intestinal mucosa is impaired in hepatocyte growth factor activator-deficient mice, Gastroenterology 127 (5) (2004) 1423–1435.
[111] H. Kataoka, M. Kawaguchi, Hepatocyte growth factor activator (HGFA): pathophysiological functions *in vivo*, FEBS J. 277 (10) (2010) 2230–2237.
[112] K. Miyazawa, Hepatocyte growth factor activator (HGFA): a serine protease that links tissue injury to activation of hepatocyte growth factor, FEBS J. 277 (10) (2010) 2208–2214.
[113] L. Naldini, L. Tamagnone, E. Vigna, M. Sachs, G. Hartmann, W. Birchmeier, Y. Daikuhara, H. Tsubouchi, F. Blasi, P.M. Comoglio, Extracellular proteolytic cleavage by urokinase is required for activation of hepatocyte growth factor/scatter factor, EMBO J. 11 (13) (1992) 4825–4833.
[114] M. Peek, P. Moran, N. Mendoza, D. Wickramasinghe, D. Kirchhofer, Unusual proteolytic activation of pro-hepatocyte growth factor by plasma kallikrein and coagulation factor XIa, J. Biol. Chem. 277 (49) (2002) 47804–47809.
[115] S. Santamaria, R. de Groot, ADAMTS proteases in cardiovascular physiology and disease, Open Biol. 10 (12) (2020) 200333.
[116] A.A. Capehart, Proteolytic cleavage of versican during limb joint development, Anat. Rec. 293 (2) (2010) 208–214 Hoboken.
[117] M. Shimoda, H. Yoshida, S. Mizuno, T. Hirozane, K. Horiuchi, Y. Yoshino, H. Hara, Y. Kanai, S. Inoue, M. Ishijima, Y. Okada, Hyaluronan-binding protein involved in hyaluronan depolymerization controls endochondral ossification through hyaluronan metabolism, Am. J. Pathol. 187 (5) (2017) 1162–1176.
[118] T. Dokoshi, L.J. Zhang, F. Li, T. Nakatsuji, A. Butcher, H. Yoshida, M. Shimoda, Y. Okada, R.L. Gallo, Hyaluronan degradation by Cemip regulates host defense against staphylococcus aureus skin infection, Cell Rep. 30 (1) (2020) 61–68 e4.
[119] C.M. Doherty, R. Visse, D. Dinakarpandian, D.K. Strickland, H. Nagase, L. Troeberg, Engineered tissue inhibitor of metalloproteinases-3 variants resistant to endocytosis have prolonged chondroprotective activity, J. Biol. Chem. 291 (42) (2016) 22160–22172.
[120] L. Chung, K. Shimokawa, D. Dinakarpandian, F. Grams, G.B. Fields, H. Nagase, Identification of the (183) RWTNNFREY(191) region as a critical segment of matrix metalloproteinase 1 for the expression of collagenolytic activity, J. Biol. Chem. 275 (38) (2000) 29610–29617.
[121] S. Tyanova, T. Temu, P. Sinitcyn, A. Carlson, M.Y. Hein, T. Geiger, M. Mann, J. Cox, The Perseus computational platform for comprehensive analysis of (prote)omics data, Nat. Methods 13 (9) (2016) 731–740.
[122] E.H. Mogensen, E.T. Poulsen, I.B. Thogersen, K. Yamamoto, A. Bruel, J.J. Enghild, The low-density lipoprotein receptor-related protein 1 (LRP1) interactome in the human cornea, Exp. Eye Res. 219 (2022) 109081.
[123] J.D. Ashcom, S.E. Tiller, K. Dickerson, J.L. Cravens, W.S. Argraves, D.K. Strickland, The human alpha 2-macroglobulin receptor: identification of a 420-kD cell surface glycoprotein specific for the activated conformation of alpha 2-macroglobulin, J. Cell Biol. 110 (4) (1990) 1041–1048.